

Chapter 6: CO₂-rich melts in the Earth

Gregory Yaxley¹, Sujoy Ghosh², Ekaterina Kiseeva³, Ananya Mallik⁴, Carl Spandler⁵, Andrew Thomson⁶, Michael Walter⁷.

1. The Australian National University, AUSTRALIA (greg.yaxley@anu.edu.au)
2. Indian Institute of Technology, Kharagpur, INDIA
3. University College, Cork, Republic of Ireland
4. Brown University, Providence RI, USA
5. James Cook University, AUSTRALIA
6. University College, London, UK
7. Carnegie Institute, Washington DC, USA

Keywords: deep carbon cycle, mantle, carbonatite, oxygen fugacity, carbon, diamond, carbonate

27 **6.1 Introduction**

28

29 Carbonate-rich magmas in the earth play a critical role in the Earth's deep carbon
30 cycle. They have been emplaced into, or erupted onto the crust as carbonatites (i.e.,
31 igneous rocks comprised of >50% carbonate minerals, with SiO₂ contents <20 wt%)
32 for the last 2.5 Ga of geological history and one volcano (Oldoinyo Lengai, Tanzania)
33 has erupted sodic carbonatite lavas since 1960¹.

34

35 Carbonate melts are inferred to exist in the upper mantle, largely on the basis of high
36 pressure experimental studies²⁻⁶. Their existence has also been inferred from the
37 mineralogy and geochemistry of some suites of peridotite xenoliths recovered from
38 alkali basalts⁷⁻⁹, and they have been observed directly in some inclusions in
39 diamonds¹⁰ and minerals in sheared garnet peridotite xenoliths¹¹. They may also be
40 present in the mantle transition zone or lower mantle in association with deeply
41 subducted, carbonate-bearing slabs¹²⁻¹⁴ and as inclusions in lower mantle diamonds¹⁵.

42

43 Because of their low density, low viscosity and ability to wet the surfaces of silicate
44 minerals in the mantle¹⁶⁻¹⁸, carbonate melts are able to migrate upwards from their
45 source regions rapidly and at extremely low melt fractions. They are able to transport
46 significant amounts of incompatible trace and minor elements, volatile elements (H₂O,
47 halogens, sulfur) as well as major components such as C, Mg, Ca, Fe, Na and K. This
48 renders them highly effective metasomatic agents and potentially major contributors
49 to fluxes of carbon between reservoirs in the deep and shallow earth. They are also of
50 particular economic importance as hosts or sources of many critical metals, including
51 the Rare Earth Elements (REE), Nb, Ta, P and others.

52

53 In this chapter, we review current understanding of the occurrence, stability and role
54 of carbonatites emplaced into or onto the earth's crust and carbonate melts in the deep
55 earth, from lower mantle to crust. We first outline constraints from high pressure
56 experimental petrology and thermodynamic considerations on their stability, as
57 functions of variables such as pressure (P), temperature (T) and oxygen fugacity
58 (fO_2). These constraints are then used in the context of different tectonic settings in
59 the Earth to infer the presence and nature of carbonate melts in those various
60 locations.

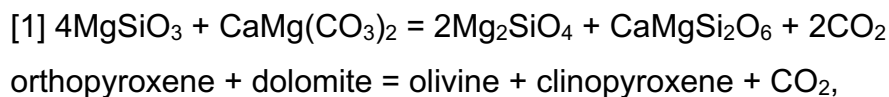
61
62
63
64
65
66
67
68
69
70
71
72
73
74
75
76
77
78
79
80
81
82
83
84
85
86
87
88
89
90
91
92
93

Carbonate melts and carbonatite magmas are also often proposed to be genetically linked to some CO₂-bearing silicate melts (melts with >20 wt% SiO₂ and dissolved, oxidised carbon, such as kimberlites, intraplate basalts, continental alkali basalts, etc) through processes such as carbonate-silicate liquid immiscibility, crystal fractionation and oxidation of diamond or graphite. Genetic relationships between carbonate melts and CO₂-bearing silicate melts in appropriate settings are also considered in this Chapter.

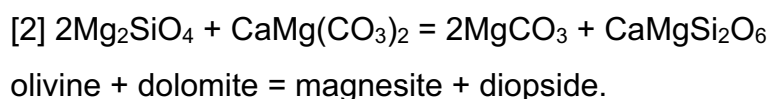
6.2 Constraints on carbonate stability in the earth's mantle

Critical to the stability, distribution, movement and capacity for mass transport of carbonate melts at mantle pressure and temperature conditions is the oxygen fugacity (fO_2) of the ambient mantle. This intensive variable exerts a very strong control on the speciation of C in the mantle, which can range from highly reduced metal carbides, to methane-fluids, to crystalline graphite or diamond, to oxidised carbon species such as CO, CO₂ or CO₃²⁻ in fluids or melts¹⁹.

The various species of carbon in peridotite upper mantle are further limited by pressure-temperature- fO_2 conditions relative to (1) the univariant graphite/diamond phase transition, (2) redox dependent reactions such as EMOD and EMFFD (see below), (3) the carbonate peridotite (or eclogite) solidus, and (4) decarbonation reactions involving carbonate minerals or carbonate in melts, and silicate phases, such as



and (5) fluid absent equilibria such as



94 For example, the stability of carbonate phases versus diamond in a melt or fluid-free,
95 Ca-poor, magnesite harzburgite assemblage is limited in P- fO_2 space by the
96 “EMOG/D” reaction [5] (enstatite-magnesite-olivine-graphite/diamond)^{20,21}:

97



99 orthopyroxene + carbonate = olivine

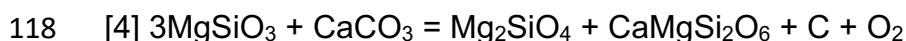
100

101 At depths from around 40 km to 240 km on a typical cratonic geotherm, the univariant
102 reaction will increase slightly in fO_2 from about -1.2 log units below FMQ to about -0.5
103 log units below FMQ²¹. At fO_2 s above this reaction, CO₂-fluid, dolomite or magnesite
104 will be stable depending on pressure relative to reactions [1] and [2]. At fO_2 s below it,
105 graphite or diamond will be stable, depending on pressure relative to the univariant
106 graphite-diamond reaction²² which lies at a pressure corresponding to about 150 km
107 depth on a cratonic geotherm. The majority of kimberlite-borne garnet peridotite
108 xenoliths for which fO_2 has been determined lie below EMOG/D, consistent with the
109 sampling of diamond by deeply sourced kimberlites passing through the cratonic
110 lithosphere. This also means that carbonate melts are unlikely to be stable at depths
111 throughout most of the cratonic mantle lithosphere, except in minor volumes (perhaps
112 adjacent to conduits for kimberlites) where metasomatic enrichment processes may
113 have locally oxidised the wall-rock significantly²³.

114

115 In carbon-bearing lherzolite assemblages, the EMFDD reaction [4] limits carbonate
116 stability in P-T- fO_2 space.

117



119 orthopyroxene + carbonate = olivine + diopside + diamond/graphite

120

121 At 5 GPa, this reaction lies at about -1.2 log units at 500°C, decreasing to -1.5 log
122 units at 1300°C, for realistic activities of the various components²⁰.

123

124 Melting of carbon-bearing peridotite to form melts with high activities of carbonate
125 therefore will be restricted to those regions of the peridotitic upper mantle where
126 oxidation state is consistent with carbonate stability, i.e. where fO_2 lies above the
127 appropriate limiting reaction at given pressure and temperature.

128 The magnitude and variation of fO_2 in the mantle has been the subject of many studies
129 over recent decades. These have used measurements by a variety of techniques (wet
130 chemical methods, Mössbauer spectroscopy, flank method, Fe K-edge μ XANES) of
131 $Fe^{3+}/\Sigma Fe$ in phases in peridotite xenoliths (spinel, garnet, pyroxenes) from the upper
132 mantle, synchrotron Mössbauer measurements of Fe^{3+} in majoritic garnets from the
133 sub-lithospheric upper mantle or mantle transition zone²⁴, $Fe^{3+}/\Sigma Fe$ measurements on
134 primitive MORB glasses^{25,26} coupled with high pressure experimental and
135 thermodynamic calibrations of relevant redox controlling reactions²⁷⁻²⁹. These studies
136 indicate that it is likely that carbonate stability in peridotite is generally limited to
137 relatively shallow parts of the continental lithosphere (i.e. depths < ca. 100km) (see
138 Section 6.6.2 for more details). In the next section, we review high pressure
139 experimental constraints on the melting of carbonate peridotite.

140

141 **6.3 Experimental constraints on the melting of carbonate peridotite in the mantle**

142

143 Many high pressure experimental studies have investigated the phase and partial
144 melting relations of (oxidised) carbonate-bearing mantle lithologies peridotite at upper
145 mantle pressures^{3,5,6,30-41}. The stable species of carbonate in sub-solidus peridotite
146 upper mantle is controlled by some key carbonate-silicate reactions. These include
147 reactions [1], [2] and [5]

148



150 forsterite enstatite magnesite

151

152 These reactions have been delineated using high pressure experiments in the CaO-
153 MgO-SiO₂±H₂O (CMS±H) system⁴²⁻⁴⁹.

154

155 In more complex natural systems, in particular containing Fe and alkali metal
156 components, reaction [4] intersects the peridotite+CO₂ system at the carbonate
157 solidus at about 2.1 GPa and 1030°C (Hawaiian Pyrolite + 5 wt% dolomite³⁰), dividing
158 the shallow sub-solidus lithospheric mantle into a shallower zone in which crystalline
159 carbonate is unstable at the expense of CO₂ fluid and a deeper zone in which dolomite
160 crystallises as part of a spinel or garnet lherzolite assemblage. At the solidus, this
161 reaction forms an approximately isobaric solidus ledge. At pressures greater than the

162 ledge is a near-solidus field of sodic dolomitic carbonate melt in equilibrium with
163 lherzolite residue. At pressures below the ledge, CO₂-rich fluid coexists with spinel
164 lherzolite.

165

166 This reaction may act as a barrier to migration of carbonate melts formed at higher
167 pressures than reaction [1] to shallower depths in continental settings where
168 geotherms are likely to intersect it. Dolomitic carbonate melts are predicted to react
169 according to reaction [1] and this may lead to elimination of the melt and crystallisation
170 of secondary clinopyroxene and olivine at the expense of orthopyroxene, and in
171 extreme cases, conversion of harzburgite or lherzolite mantle to orthopyroxene-free,
172 clinopyroxene-rich wehrlite along with liberation of a CO₂-rich fluid. Such a process
173 was inferred to have occurred in some spinel wehrlite xenoliths hosted in the Newer
174 Volcanics of Victoria, southeastern Australia^{8,50} and in the Olmani Cinder cone,
175 northern Tanzania⁵¹. It has been suggested that only in the circumstance where
176 magma conduits become armoured with orthopyroxene-free wehrlite are dolomitic
177 carbonatites able to ascend to pressures less than the solidus ledge, potentially
178 entering the crust, evolving to more calcic compositions and in some cases becoming
179 emplaced in the crust or erupted⁵².

180

181 In oceanic settings, convective geotherms are at higher temperatures than conductive
182 geotherms in continental lithosphere and are not expected to intersect the solidus
183 ledge or reaction [1].

184

185 At higher pressures (3.4 GPa, 1080°C)³⁰, the vapour absent reaction [2] intersects the
186 peridotite solidus, dividing the subsolidus regime into a lower pressure field of dolomite
187 garnet lherzolite and a higher pressure field of magnesite garnet lherzolite.

188

189 Low degree partial melts in experimentally investigated peridotite-CO₂±H₂O systems
190 with natural compositions are generally broadly alkali-rich and calcio-dolomitic to
191 dolomitic in composition³. Solidus temperatures are considerably lower than volatile
192 free systems, and although experimental studies which include CO₂ and H₂O are
193 relatively rare, available evidence suggests solidus temperatures are even lower^{3,53}.

194

195 In the following sections, we apply the experimental and other constraints to infer the
196 existence and behaviour of carbonate melts in different tectonic settings.

197

198 **6.4 Carbonate melts associated with subduction zones.**

199

200 The mantle is believed to have played a key role in controlling the long-term carbon
201 budget in the exosphere through cycling of carbon from the surface to the mantle and
202 back again^{6,54,55}. The deep carbon cycle is regulated at the surface by the quantity of
203 carbon subducted into the mantle at convergent margins and by volcanic degassing
204 of mantle-derived melts releasing carbon to the exosphere at mid-ocean ridges, ocean
205 islands and arc volcanoes. A substantial proportion of the mass of carbon drawn into
206 the mantle at subduction zones, (anywhere between 20 and 100% is recycled back to
207 the surface via fore-arc degassing and arc magmatism⁵⁶, as discussed in detail in
208 Chapter 12 of this volume. Estimates of the net annual flux of carbon ingassing and
209 outgassing via these processes are difficult to constrain with certainty, and range from
210 negligible values to ~60 Mton/year net recycling^{6,56}.

211

212 Carbon enters the mantle at subduction zones in sediments, altered oceanic crust and
213 mantle lithosphere, with total input flux in the range of ~ 50 to 100 Mt/year at modern
214 subduction zones^{6,56}. Sedimentary carbon includes both biogenic organic carbon and
215 carbonate. In more than a third of studied modern subduction zones carbonate-rich
216 materials make up a substantial fraction of the down-going sediment, whereas in
217 others it is absent altogether (e.g. refs^{57,58}). However, organic carbon is expected to
218 be at least a minor component in pelagic sediments and turbidites⁵⁶.

219

220 Carbon is deposited during hydrothermal processes at mid-ocean ridges where
221 carbonate (calcite and aragonite) forms during alteration of oceanic crust by reaction
222 with CO₂ in seawater; biotic organic carbon in oceanic crust is minor relative to abiotic
223 organic compounds and inorganic carbonates. The top few hundred meters of oceanic
224 crust contain an average of ~2.5 wt.% CO₂ and at deeper levels the carbon content,
225 mostly in the form of organic hydrocarbon species, drops below 0.2 wt.% throughout
226 the remainder of the crustal section. Altered lithospheric mantle that is exposed to
227 alteration by seawater also carries carbonate, although likely at an overall fraction
228 much less than that of oceanic crust^{56,59}.

229

230 Down-going slab materials never reach temperatures high enough for “dry” partial
231 melting during blueschist- and eclogite-facies metamorphism at fore-arc depths (up to
232 ~80 km)^{60,61}, and portions of the slab that do not experience pervasive dehydration
233 can effectively transport carbon to greater depths into the mantle. Nevertheless, at
234 pressures above ~ 0.5 GPa, carbonate solubility in aqueous fluids increases with
235 temperature⁶², so fluids produced by metamorphic devolatilisation of the slab can be
236 effective at dissolving carbonate minerals and mobilising carbon⁶³. Much of this carbon
237 may be redistributed within the slab⁶⁴ or sequestered into serpentinised mantle rock
238 that overlies the slab⁶⁵⁻⁶⁷, some of which in turn is dragged down with the descending
239 slab.

240

241 At sub-arc depths (80 to 200 km) slab surface temperatures reach between 600 and
242 1000°C⁶⁸, and carbonate mineral dissolution becomes much more efficient due to
243 higher solubilities in hydrous fluids⁶⁹ and silicate melts⁷⁰ at these depths. In some
244 cases, carbonatite liquids may also form via fluid-flux melting of carbonate-rich
245 metasedimentary rocks⁷¹ or carbonate-bearing metagabbros⁷². As a consequence,
246 CO₂ (± CO₃²⁻)-rich fluid phases migrating from the downgoing slab, or from buoyantly
247 upwelling slab diapirs^{73,74}, can introduce a significant carbon flux from the slab to the
248 overlying mantle wedge. Evidence in support of C-rich fluid phases at the slab surface
249 comes from garnet and clinopyroxene inclusions in diamonds from Dachine, South
250 America, which have major and trace element characteristics indicating growth at the
251 surface of a subducting slab at ~200 km depth, possibly in metalliferous
252 metasediment⁷⁵.

253

254 Slab-derived fluids migrating into the overlying mantle will experience progressive
255 heating as they ascend through the inverted temperature gradient of the mantle
256 wedge⁷⁶ (Figure 1). The introduction of C-O-H fluids or melts results in a significant
257 lowering of wedge peridotite solidus, such that carbonatite liquids can be produced at
258 temperatures below 950 °C⁷⁶. Such carbonatitic liquids (+H₂O) are expected to be
259 highly mobile but will react with the wedge upon ascent and heating, to produce
260 carbonated hydrous silicate melts (>1020 °C; refs^{74,76}). Further ascent will favour
261 further peridotite melting, increasing melt fractions and diluting dissolved volatile
262 contents. Upwelling from the hot core of the wedge may impart retrograde melt-rock,

263 or fluid-rock reactions, locking some carbonate (+H₂O) phases in the mantle
264 lithosphere and lower crust⁵⁶, but most volatile flux from the slab is expected ultimately
265 to be delivered to the upper arc crust via fractionating and degassing arc magmas.

266

267 *Figure 1*

268

269 The unique petrophysical evolution of magmas traversing the mantle wedge means
270 that carbonatitic liquids are unable to be tapped from the mantle to the surface, which
271 explains the lack of carbonatites found in supra-subduction zone settings⁷⁷. Further,
272 carbonated sub-arc mantle lithosphere and arc lower crust may eventually be
273 preserved as subcontinental lithosphere through reaction of volatile-rich melts with the
274 mantle⁷⁸, or recycled into the convecting mantle; possibly thereafter to undergo
275 melting to produce carbonatites in intraplate settings.

276

277 ***6.5 Melting of subducted, carbonated sediment and ocean crust in the deep*** 278 ***upper mantle and transition zone***

279 Whilst subduction to ~ 200 km depth can remove a significant fraction of the initial
280 down-welling carbon flux to the mantle wedge, experimental evidence of carbonate
281 stability, modelling of phase equilibria and slab devolatilization indicate that in some
282 subduction zones a substantial portion of subducted carbon or carbonate may make
283 it past the dehydration zone and into the deeper mantle^{79,80}. Experiments also suggest
284 that carbonate may be reduced to elemental carbon (graphite or diamond) at depths
285 shallower than 250 km in more reducing eclogitic assemblages, although for oxidation
286 states typical of MORB (e.g. ref⁸¹) eclogitic assemblages should remain in the
287 carbonate stability field to at least 250 km²⁸.

288

289 Inclusions of carbonate minerals in superdeep diamonds provide the strongest direct
290 evidence for a carbonate component subducted past the volcanic front and at least to
291 transition zone depths⁸²⁻⁸⁵. In addition, the distinctive major and trace element
292 compositions of silicate inclusions in many superdeep diamonds (e.g. majorite garnet,
293 Ca- and Ti-rich perovskite) have been interpreted to preserve a direct record in their
294 origin of a low-degree carbonated melt derived from subducted oceanic crust^{83,86,87}.
295 Both the carbon isotopic composition of the diamonds and the oxygen isotope

296 composition of inclusions provide further evidence for a key role of subducted crustal
297 components in the origin of many superdeep diamonds and their inclusions^{88,89}. Thus,
298 it seems that melting of carbonated sediment and oceanic crust in the deep upper
299 mantle and transition zone may play a key role in the deep carbon cycle.

300

301 Figure 2 compares the solidus determinations from published studies on the melting
302 behaviour of carbonated pelitic sediment and carbonated oceanic crust at upper
303 mantle and transition zone conditions. The solidus of carbonated pelitic sediment was
304 determined by Tsuno and Dasgupta⁹⁰ at 2.5 to 3 GPa and by Grassi and Schmidt⁹¹ at
305 8 to 13 GPa, with melts ranging from granitic at low pressures to K-rich carbonatitic at
306 higher pressures. On the basis of solidus determinations in these studies only in the
307 hottest subduction zones would melting of anhydrous carbonated sediments occur in
308 the sub-arc region. The addition of water reduces the solidus of pelitic sediments, but
309 unless sediments are water saturated, perhaps by fluxing of water-rich fluids from
310 below, carbonated slab sediments may reach the deep upper mantle and transition
311 zone⁹². At higher pressures approaching the transition zone, the experiments of Grassi
312 and Schmidt⁹¹ indicate that carbonated sediments can melt along warm and hot slab-
313 top geotherms, but colder slabs could transport sedimentary carbonate into the deeper
314 mantle (Figure 2).

315

316 *Figure 2*

317

318 There have been many experimental studies of melting carbonated basaltic
319 compositions, both in simplified^{93,94} and natural systems^{12,13,35,95-98}. The small number
320 of phases in basaltic compositions hampers studies in simplified compositions,
321 whereas subtle compositional dependencies hamper studies on natural compositions
322 Indeed, subtle variations in bulk compositions between studies (Table 1) likely cause
323 the significant variations in position and shape of the carbonated basalt solidus (e.g.
324 refs^{13,99}.

325

326 In the lower pressure range (e.g. <3-5 GPa) a carbonate phase is not always stable at
327 the solidus depending on the bulk CO₂ and SiO₂ contents. In those with higher
328 SiO₂/CO₂ ratios, CO₂ and/or silicate melts containing dissolved CO₂ define the

329 solidus^{13,96,98}, whereas compositions with lower SiO₂/CO₂ observed carbonate stability
330 and carbonate melt production along the solidus from low pressure^{13,35,99,100}.
331 Additionally, near-solidus melts have been identified with a wide range of composition
332 from mafic to silicic. In some case silicate melts are observed at the solidus before
333 carbonate melts whereas in other cases this relationship is reversed, and both kinds
334 of melts have been interpreted to coexist together as immiscible liquids^{12,100,101}. The
335 observation of immiscible melts may reflect the maximum CO₂ solubility in silicate
336 melts, and the appearance of liquid immiscibility will therefore depend on the CO₂
337 content of the bulk composition.

338

339 At higher pressures of the deep upper mantle and transition zone, starting
340 compositions again show a remarkable control on melting behaviour (Figure 2). When
341 comparing the carbonated starting compositions used in the various studies, there are
342 considerable differences, perhaps most notably in SiO₂ and CO₂ contents, and Ca#.
343 Thomson et al.¹³ observed that the Ca# has an important control on the stable
344 carbonate phase at the solidus beyond the pressure of dolomite breakdown (> ~10
345 GPa). Phase relations apparently preclude coexistence of magnesite and aragonite in
346 majorite and clinopyroxene bearing assemblages, and which of these carbonate
347 phases is stable has an important control on the solidus shape and melt compositions.

348

349 In Ca-rich carbonated basalt bulk compositions the stable phase is aragonite which is
350 also a host for sodium¹². However, in lower Ca# bulk compositions magnesite is stable,
351 and because sodium is relatively insoluble in magnesite, another Na-rich carbonate
352 stabilizes in the subsolidus assemblage at pressures greater than ~15 GPa. The
353 appearance of a Na-carbonate phase in the sub-solidus produces a dramatic lowering
354 of the melting temperature and a deep trough along the solidus between ~10 and 15
355 GPa that is not observed where aragonite is stable (Figure 2). When Na-carbonate
356 occurs on the solidus it is observed that the melting temperature at pressures > ~15
357 GPa (~1150 C) is indistinguishable from that observed for a simplified Na-carbonate-
358 rich bulk composition at these conditions¹⁰² (Figure 2). As the majority of natural
359 MORB compositions, fresh and altered, fall to the Mg-rich side of the majorite-
360 clinopyroxene join they should have magnesite and not aragonite as the stable
361 carbonate at high pressures, and experience the lowered solidus at transition zone
362 conditions¹³.

363

364 Figure 3 shows melt compositions projected onto a plane differentiating major and
365 minor components of sediment and basalt-derived carbonated melts, demonstrating a
366 generally continuous evolution with increasing pressure and temperature. The lowest
367 degree melts of carbonated basalt are highly calcic, even when the sub-solidus
368 carbonate is magnesite, because magnesite is the liquidus phase in most carbonate
369 systems¹⁰². Carbonated melts are enriched in incompatible elements and have high
370 concentrations of TiO₂, P₂O₅ and alkalis (Na₂O and K₂O), the relative abundances of
371 which will be controlled by the bulk composition of the protolith. Sediment melts are
372 dominated by potassium, whereas melts from carbonated basalt have alkali contents
373 that are dominated by Na₂O. Melt Na₂O content increases systematically with
374 pressure in basaltic compositions, resulting from the decreasing compatibility of Na₂O
375 in the coexisting residual phase assemblage. Thomson et al.¹³ observed that melt
376 compositions of carbonated basalt in the transition zone remain approximately
377 constant over a wide temperature interval of >300 °C above the solidus, and only when
378 temperature exceeds ~1,500°C does the silica content of the melt increase. This
379 behaviour is reminiscent of the melting behaviour observed in carbonated peridotite
380 assemblages at lower pressure¹⁰³.

381

382 *Figure 3*

383

384 **6.6 Carbonate melts and kimberlites in the cratonic lithospheric mantle**

385

386 Cratonic mantle lithosphere underlies ancient, continental blocks which have been
387 geologically stable for billions of years. It is chemically depleted, thick and buoyant.
388 Unlike other tectonic settings, any surface expression of cratonic magmatism is
389 manifested by emplacement of small volume, rare, exotic, volatile-rich alkali- and
390 carbonate-rich magmas, such as carbonatites, kimberlites, lamproites, lamprophyres
391 various and other highly silica-undersaturated magmas^{104,105}, all of which have a deep
392 mantle origin. Describing the detailed petrology of these rocks is beyond the scope of
393 this study, and the reader is referred to the work of Jones et al.⁷⁷. Below we give a
394 short overview of an important carbonate-bearing silicate volcanic rock found in
395 cratonic settings: kimberlites.

396

397 6.6.1 Kimberlites

398 **Kimberlites** are volatile- (chiefly CO₂-) rich, silica-poor alkaline, ultrabasic magmas
399 generally believed to be derived from a depth of ≥150–250 km and almost exclusively
400 emplaced into cratonic crust. Kimberlite magmas are economically significant because
401 of their association with diamonds. They have been subdivided into two major groups
402 on the basis of petrographic and geochemical characteristics: Group 1 kimberlites and
403 Group 2 kimberlites¹⁰⁶⁻¹⁰⁸. Group 1 kimberlites are CO₂-rich, potassic, ultrabasic rocks
404 with a typical porphyritic texture, with large phenocrysts of most commonly olivine
405 surrounded by a fine-grained matrix consisting of olivine, phlogopite, spinel, ilmenite,
406 monticellite, calcite, apatite, perovskite and other phases¹⁰⁹. Group 2 kimberlites, or
407 orangeites, are restricted to southern Africa. However, similar rocks have also been
408 identified in Australia, India, Russia and Finland. They are texturally similar to the
409 Group 1, but have distinct compositional and isotopic differences, manifested mainly
410 by the presence of phlogopite, K-Ba-V titanites and Zr-bearing minerals, such as
411 kimzeytic garnets¹⁰⁹ lower ϵ_{Hf} and ϵ_{Nd} values, and high radiogenic ⁸⁷Sr isotope
412 compositions¹¹⁰.

413

414 Similar to carbonatites, kimberlites are volumetrically very minor but are widespread
415 throughout the cratonic parts of continents, with the latest discoveries extending the
416 Gondwanan Cretaceous kimberlite province to Antarctica¹¹¹. The main difference with
417 carbonatites though, is in their origin in subcratonic lithospheric or asthenospheric
418 mantle enriched by an ocean island basalt source in the case of Group I kimberlites,
419 whereas Group II kimberlites are derived from metasomatized lithospheric
420 mantle^{108,112}, and their eruption predominantly through stable parts of cratons¹¹³. To
421 our knowledge, there are no reported occurrences of kimberlites in the oceanic
422 crust^{113,114}.

423

424 The accurate determination of the kimberlite parental magma composition and its
425 origin is hampered by the ubiquitous presence of a large fraction of foreign materials
426 (mantle and crustal xenocrysts and xenoliths), in particular olivine crystals, collected
427 from lithospheric mantle during their ascent to the surface, and by low temperature
428 alteration during and after emplacement. Petrological studies of the unaltered
429 Udachnaya kimberlite pipe in the Siberian Craton showed high enrichment in CO₂,

430 halogens and alkalis and resulted in a hypothesis in which genetic links between
 431 kimberlites and carbonatites were important^{115,116}. Later, experimental studies
 432 concluded that magmas potentially parental to kimberlites originate as dolomitic
 433 carbonate liquids in metasomatized, oxidised zones in the deep cratonic lithospheric
 434 mantle²³ that segregate and become progressively more silicate-rich due to the
 435 assimilation of silicate material (mostly orthopyroxene) during ascent through
 436 refractory lithosphere during their ascent¹¹⁷.

437

438 Alternative models are based on high pressure experimental studies of estimated
 439 compositions of melts parental to kimberlites and have attempted to identify pressure,
 440 temperature and volatile conditions at which the melts are multiply saturated in garnet
 441 peridotite phases^{118,119}. Such studies have indicated that the most likely source for
 442 kimberlite parental melts is hydrous, carbonate-bearing garnet harzburgite in the deep
 443 cratonic lithospheric mantle or sub-lithospheric asthenosphere.

444

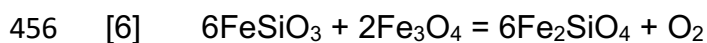
445 In either case, kimberlite genesis clearly requires a mantle sufficiently oxidised for
 446 crystalline carbonate (Ca-magnesite) to be stable in the peridotitic source²³, and the
 447 source is constrained to be greater than ≈ 150 km depth in cratonic lithospheric mantle
 448 because of the presence of xenocrystic diamonds.

449

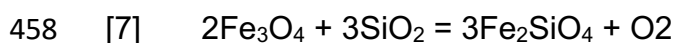
450 *6.6.2 Redox constraints on carbonate stability in the cratonic lithospheric mantle.*

451 In any volume of the cratonic mantle, in the absence of externally derived melts or
 452 fluids, the local oxygen fugacity is controlled by silicate or oxide mineral exchange
 453 equilibria such as reactions [6] to [9], which involve oxidation of Fe²⁺-bearing
 454 components and reduction of Fe³⁺-bearing components.

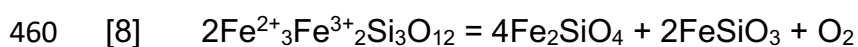
455



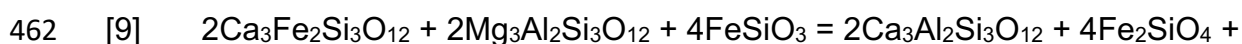
457 opx spinel olivine



459 spinel opx/olivine olivine



461 garnet olivine opx



463 garnet garnet opx garnet olivine

464 $6\text{MgSiO}_3 + \text{O}_2$

465 opx

466

467 For example, reactions [6] to [9] have been calibrated experimentally^{21,27,120-122},
468 meaning that in principle, the oxygen fugacity of a spinel or garnet peridotite from the
469 upper mantle can be determined if the activities of the Fe-bearing components in the
470 minerals that contain Fe^{2+} and Fe^{3+} can be determined, along with other mineral
471 component activities, pressure and temperature.

472

473 These experimental calibrations can be combined with conventional thermobarometry
474 to calculate the variation in $f\text{O}_2$ as a function of depth in the peridotite lithospheric
475 upper mantle, as recorded by peridotite xenoliths from kimberlites in the case of
476 cratonic mantle lithosphere, for example. The uppermost cratonic mantle lithosphere,
477 based on spinel peridotite xenoliths sampled by kimberlites has $f\text{O}_2$ between 0 and -
478 1 log units relative to FMQ for primitive ($\Delta\log f\text{O}_2^{\text{FMQ}}$)¹²³, well within the carbonate
479 stability field. In the garnet peridotite facies, $f\text{O}_2$ decreases systematically with
480 increasing pressure (depth) through the cratonic lithosphere^{23,123,124} (Figure 4),
481 although the xenolith record exhibits complications associated with oxidative
482 overprinting associated with metasomatism, particularly at depths >150 km.
483 Decreasing $f\text{O}_2$ with increasing depth is expected on a thermodynamic basis, because
484 of the molar volume changes of reactions such as [8] and [9]^{27,125}. It is therefore likely,
485 that melts with high carbonate activities are unstable relative to graphite or diamond
486 at depths greater than approximately 90-120 km in the cratonic lithospheric mantle.

487

488 *Figure 4*

489

490 At depths around 250-300 km, the $f\text{O}_2$ -P path is expected intersect the Ni precipitation
491 curve, an FeNi alloy will exsolve from peridotite and $f\text{O}_2$ will be buffered near the iron-
492 wüstite (IW) buffer deeper into the upper mantle. In the presence of metallic FeNi alloy,
493 some reduced carbon will be accommodated as (Fe,Ni) carbides. Rohrbach et al.¹²⁶
494 have calculated that, assuming the mantle contains 50-700 ppm FeNi and 50-500 ppm
495 C at 300 km depth, it would contain an assemblage of $(\text{Fe,Ni})_3\text{C} + \text{FeNi alloy} +$
496 diamond or an Fe-Ni-S-C melt¹²⁷.

497

498 Although the cratonic mantle becomes more reduced with increasing depth, local
499 redox heterogeneities may be introduced, particularly at depths greater than 150 km,
500 by metasomatic fluids such as carbonate-bearing silicate melts^{23,128} with low
501 carbonate activities ²¹, possibly derived from the asthenosphere or from oxidised
502 crustal material recycled via subduction. In some cases, the degree of oxidation in the
503 lower part of the cratonic lithospheric upper mantle could be sufficient to stabilise
504 crystallisation of carbonates (magnesite in peridotite) which, in the presence of H₂O
505 could melt and produce magmas parental to kimberlites^{118,119}.

506

507 *6.6.3 The involvement of carbonate melts in metasomatism of the deep cratonic* 508 *lithospheric mantle*

509 Apart from carbonatites and kimberlites that were emplaced into or erupted onto the
510 crust, CO₂-rich fluids, carbonate melts or carbonated silicate melts are often inferred
511 to be major agents of mantle metasomatism and trace element enrichment in the
512 lithospheric mantle. Unlike, for example, alpine massifs, most peridotite and eclogite
513 xenoliths carried to the surface by kimberlites are chemically enriched relative to the
514 depleted lithospheric mantle. It may be that the degree of this enrichment was
515 previously severely underestimated^{113,129} and that CO₂-rich metasomatism is a wide-
516 spread process throughout the cratonic mantle.

517

518 It is not always easy to distinguish and characterise the exact nature of a particular
519 metasomatic overprint observed in natural rocks. Given Giga-year ages of the cratonic
520 lithospheric mantle, there is a likelihood of multiple melting (i.e. depletion) and
521 subsequent re-enrichment events. Moreover, the challenge of deciphering a particular
522 metasomatic event in a given mantle xenolith is exacerbated by the possibility of
523 multiple types of percolating fluids. For instance, in addition to the carbonatitic CO₂-
524 rich metasomatism, an H₂O-rich alkali silicate metasomatism, perhaps, of a proto-
525 lamproite type has been reported¹³⁰⁻¹³².

526

527 At the reduced conditions likely to exist in much of the deep cratonic lithospheric
528 mantle and underlying asthenosphere, carbonate phases are not expected to be
529 generally stable and so melts with high carbonate activities such as carbonatites will
530 likely not form, except locally in localised zones already strongly oxidised due to earlier

531 metasomatism²³. Carbon transport will likely be as low activity carbonate dissolved in
532 undersaturated silicate melts²¹, or as CH₄+H₂O fluids^{129,133,134}. However, it should also
533 be noted that the depth-*f*O₂ profile of the asthenospheric mantle is not necessarily the
534 same as that observed in xenoliths studies from the cratonic mantle or inferred from
535 thermodynamic calculations. Based on CO₂-Ba-Nb systematics of oceanic basalts the
536 convecting mantle may in fact be considerably more oxidised at pressures greater
537 than about 3 GPa¹³⁵.

538

539 If undersaturated silicate melts with dissolved carbonate or CO₂ at low activities form
540 as a result of adiabatic upwelling in plumes or rifts, segregate from their
541 asthenospheric sources and percolate upwards into parts of the cooler, deep cratonic
542 lithosphere they will freeze into the lithospheric mantle as the appropriate peridotite +
543 volatile solidus is locally crossed. Oxidized carbon species will be exsolved from the
544 melt during crystallisation and would reduce to C or CH₄ (CO₂ = C + O₂; CO₂ + 2H₂O
545 = CH₄ + 2O₂) because of the low ambient *f*O₂ in the deep cratonic lithosphere. Fe²⁺
546 in the melt and the wall rock will oxidize to Fe³⁺ (2FeO + 1/2 O₂ = Fe₂O₃) and be
547 incorporated into garnet and pyroxenes, leading to the observed increase in
548 lithospheric *f*O₂ associated with metasomatism. The increased activity of H₂O may
549 cause a decrease in solidus temperatures of peridotite locally and lead to partial
550 melting in a process known as hydrous redox melting. Only after sufficient oxidation
551 by this type of metasomatic process could the *f*O₂ of the deep cratonic lithospheric
552 mantle be raised sufficiently to allow carbonate stability and the formation of
553 carbonatites, kimberlites and related rocks at these depths.

554

555 ***6.7 Carbonate melts beneath ocean islands in intraplate settings***

556

557 Observations from natural samples indicate the role of CO₂, specifically CO₂-rich
558 silicate melts, in the metasomatism of the upper mantle beneath ocean islands in
559 intraplate settings. Carbonate phases, interpreted to be quenched carbonate liquids,
560 have been identified in metasomatized harzburgite xenoliths in Kerguelen and Canary
561 Islands^{136,137}. These carbonate inclusions are texturally associated with silicate glass
562 inclusions, either as globules within a silicate matrix, or as intimate associations with
563 silicate inclusions. Such textural associations between the carbonate-rich phases and
564 the silicate glasses have led to the conclusion that the carbonate-rich phases are

565 products of immiscibility of a single carbonated silicate melt phase which exists at
566 depth, possibly at upper mantle conditions. Geochemical modelling of rejuvenated
567 Hawaiian lavas also indicates the presence of carbonate-rich liquids in the source of
568 these lavas¹³⁸.

569

570 *6.7.1 How do CO₂-rich silicate melts form in the upper mantle? Can these CO₂-rich*
571 *melts explain the chemistry of erupted magmas in intraplate ocean islands?*

572 Previous experimental studies have demonstrated that CO₂-rich silicate melts can be
573 produced in upper mantle conditions as follows. Carbon may exist in its oxidized form
574 as carbonate mineral or as liquid in the mantle at oxygen fugacities that are about 2
575 log units higher than that of the Iron-Wüstite buffer [given by equilibrium [10]

576

577 [10] 2Fe + O₂ = 2FeO

578 iron wüstite

579

580 which corresponds to depths above 150-250 km^{21,139} in oceanic lithosphere.
581 Carbonate may be present deeper in the mantle in locally oxidized regions^{140,141}. Due
582 to cryoscopic depression of freezing point, carbonate-bearing lithologies (peridotite
583 and recycled oceanic crust or eclogite) have lower solidus temperatures than
584 nominally anhydrous or carbonate-free lithologies, as demonstrated by experimental
585 studies^{5,33,47,95-97,100,142-149}. This implies that in an upwelling mantle, partial melting of
586 carbonated lithologies is initiated deeper than the surrounding carbonate-free
587 lithologies. Near-solidus partial melting of carbonated peridotite and/or carbonated
588 recycled oceanic crust (eclogite) produces carbonatitic liquids (>25 wt.% CO₂, <20
589 wt.% SiO₂). These carbonatitic liquids tend to be very mobile owing to their low
590 viscosities and low dihedral angles¹⁵⁰, which lead to their escape from the site of
591 generation. These rising liquids can cause flux-based partial melting of peridotite and
592 eclogite in an adiabatically upwelling plume mantle in intraplate settings, which
593 produces CO₂-bearing silicate melts (Figure 5a).

594

595 *Figure 5*

596

597 Peridotite is the dominant lithology of the Earth's mantle. This increases the likelihood
598 of partial melts of CO₂-bearing peridotite being the best candidate for explaining the

599 geochemistry of ocean island basalts that commonly erupt in ocean islands in
600 intraplate settings. The next likely candidate for ocean island basalts would be partial
601 melts of CO₂-bearing eclogite, given recycled oceanic crust forms the dominant
602 chemical heterogeneity in the Earth's mantle¹⁵¹. Comparison of major element
603 chemistry of partial melts of CO₂-bearing peridotite and eclogite with natural, near-
604 primary ocean island basalts indicate that carbonated peridotite-derived partial melts
605 are too TiO₂-poor¹⁵², while carbonated eclogite-derived partial melts are too depleted
606 in MgO¹⁰⁰. Also, the peridotite derived partial melts can explain the MgO content very
607 well for the ocean island basalts, while the eclogite-derived partial melts can explain
608 the TiO₂ contents. This implies that the source of ocean island basalts would be best
609 explained by a hybrid source involving contributions from both peridotite (high MgO)
610 and eclogite (high TiO₂). A previous study indicated a couple of geodynamic scenarios
611 involving CO₂-bearing eclogite and peridotite in the source of ocean island basalts¹⁵³
612 (Figure 5b).

613

614 Deep carbonatites are formed by very low degree partial melting of carbonate-bearing
615 eclogites, that are present in deep locally oxidized upper mantle domains. These
616 carbonatites rise up and cause flux melting of overlying volatile-free eclogites. The flux
617 melting produces eclogite-derived carbonated silicate melts (ranging from basanites
618 to andesites) that are out of chemical equilibrium with their surrounding peridotite and
619 undergo reactive infiltration. The metasomatic process or melt-rock reaction
620 associated with such reactive infiltration forms ocean island basalts.

621

622 Deep carbonatites can also be generated by very low degree partial melting of
623 graphite/diamond-bearing peridotite or eclogite at the redox front (150-250 km depth,
624 where reduced carbon in the form of diamond/graphite is oxidized to a carbonatitic
625 melt). These carbonatites can cause flux-melting of volatile-free eclogite, and can
626 undergo subsequent reactive infiltration through the peridotite, as described above.

627 A question arises whether the involvement of CO₂ in the source is required for all
628 ocean island basalts. Studies have shown that basanitic ocean island basalts can be
629 explained by partial melting of volatile-free peridotite ± eclogite in the source, however,
630 more silica-undersaturated ocean island basalts such as nephelinites and melilitites
631 require the involvement of CO₂^{153,154}.

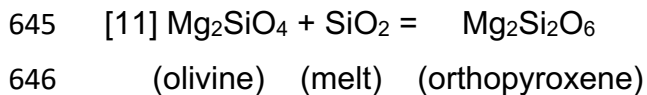
632

633 *6.7.2 Effect of CO₂ on the reaction between eclogite-derived partial melt and peridotite*
634 CO₂ dissolves in silicate melts as both molecular CO₂ and CO₃²⁻ anions. When
635 network modifying cations (those that depolymerize the silicate network) such as Na⁺,
636 K⁺, Ca²⁺, Mg²⁺ and Fe²⁺ are available in the silicate melt, CO₃²⁻ bonds with these
637 cations¹⁵⁵. These carbonate complexes result in the cations being removed from their
638 networking modifying roles. Thus, these carbonate complexes give rise to pockets of
639 polymerized networks in the silicate melt structure¹⁵⁶.

640

641 When eclogite-derived melt reacts with olivine and orthopyroxene bearing peridotite,
642 the following equilibrium [11] buffers the thermodynamic activity of SiO₂ (*a*_{SiO₂}) in the
643 reacted melt:

644



647

648 The localized separation of polymerized silicate networks and carbonate complexes
649 in the silicate melt structure result in requirement of excess free energy of mixing
650 between the two structural components. This increases the activity co-efficient of SiO₂
651 in the melt (γ_{SiO_2}). Higher γ_{SiO_2} when *a*_{SiO₂} is buffered results in decrease of mole
652 fraction of SiO₂ (*X*_{SiO₂}) in the melt¹⁵². Thus involvement of CO₂ in the melt-rock reaction
653 decreases the SiO₂ content of the product melt, driving eclogite-derived basanites and
654 andesites to produce nephelinites and melilitites (depending on the amount of CO₂
655 available in the system)^{153,154}. Higher γ_{SiO_2} and increased degree of polymerization of
656 the silicate domain of the melt network also implies that saturation of orthopyroxene is
657 preferred over the saturation of olivine in the residue of melt-rock reaction. Thus, the
658 stability field of orthopyroxene is enhanced over that of olivine^{47,152-154}. Also, cations
659 such as Ca²⁺, Mg²⁺, Na⁺ and K⁺ prefer to enter the melt structure to form carbonate
660 complexes in the presence of CO₂. This enhances the calcium, magnesium and alkali
661 contents of the product melts.

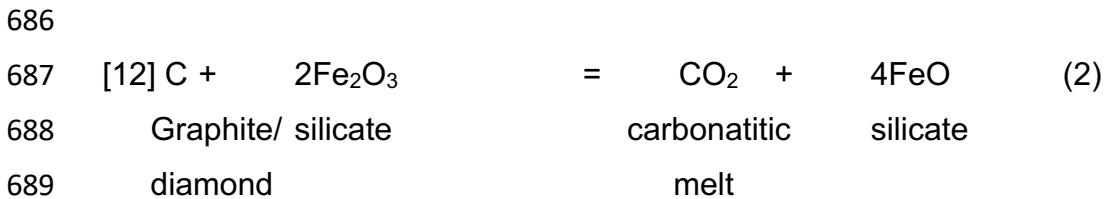
662

663 **6.8 Carbonate melts under mid-ocean ridges**

664 Along mid-ocean ridges, where divergent tectonic plates move apart from each other,
665 the rising asthenospheric mantle decompresses and partially melts to create basaltic
666 magma that buoyantly rises to the Earth's surface and solidifies to form new oceanic

667 crust. During decompression melting, volatile-free mantle lithologies melt at ~60 km
 668 producing silicate melts¹⁵⁷. Beneath ridges at shallow depths, carbonate-bearing
 669 silicate melts (basalts) are stable^{5,103,143}. Melting in carbonated mantle lithologies may
 670 take place at depths as deep as ~300-km¹⁴³ due to depression of the mantle solidus
 671 temperature^{5,29,158}.

672
 673 Figure 6 shows the stability fields of carbonates, carbonate and silicate melts in an
 674 adiabatically upwelling mantle and is compared with fO_2 of the asthenospheric mantle.
 675 The oxygen fugacity determined using reaction (1) suggests that carbonatitic melts
 676 are unstable at depths greater than 300-km due to the increase activity of Fe^{3+} -rich
 677 components in mantle minerals^{139,159,160}. At the lower end of carbon concentrations in
 678 the mantle (30 ppm C for a MORB source mantle⁵⁴ and an initial $Fe^{3+}/\Sigma Fe$ content of
 679 4 %, graphite would transform to diamond at depths of ~160 km (Fig. 2) and diamond
 680 is the stable phase instead of carbonates or carbonatitic melts^{29,123,124}. If the mantle is
 681 reduced below ~250 km depth and becomes metal saturated, then carbonatitic melt
 682 would be stable only to a depth of 150 km. During adiabatic upwelling of the upper
 683 mantle, reduction of Fe^{3+} locked in mantle silicates to Fe^{2+} , results in concomitant
 684 oxidation of diamond or graphite and results in carbonatitic melting¹³⁹. This redox
 685 process can be explained by reaction [12]:



690
 691 As soon as 30 ppm of graphite in the upper mantle is oxidized, $Fe^{3+}/\Sigma Fe$ content of
 692 the remaining mantle drops from 4 to 3 %. After such redox melting, the fO_2 of the
 693 upper mantle increases again and finally reaches the level of mid-ocean ridge basalts
 694 at around FMQ (Figure 6).

695
 696 *Figure 6*

697
 698 **6.9 Crustally emplaced carbonatites**

699 Natural carbonate melts represent a tiny proportion of magmatic rocks of the Earth's
 700 crust, but nonetheless provide important insights into mantle-to-crust carbon transfer

701 over geological time. Carbonate melts primarily refer to carbonatites, but could also
702 include kimberlites and various other alkaline mafic-ultramafic silicate magma series
703 (e.g., lamprophyres). All of these magma types have indisputable mantle origins as
704 revealed by stable and radiogenic isotope signatures, as well as a common
705 association with mantle-derived alkaline silicate magmas⁷⁷.

706

707 Carbonatites (magmatic rocks with >50% carbonate minerals) are variably classified
708 into a number of groups based on their chemistry, with most workers agreeing on at
709 least 5 groups; calcio-carbonatite, dolomite carbonatite, ferro-carbonatite, natro- (or
710 alkali-) carbonatite, and rare earth carbonatites⁷⁷. The Ca-Mg-Fe rich carbonatites are
711 primarily found as intrusive complexes that may to some extent represent crystal
712 cumulates from carbonatite magma¹⁶¹, or as melt inclusions in igneous and mantle
713 minerals^{162,163}. Extrusive carbonatites are relatively rare in the rock record¹⁶⁴ and
714 include the only known active carbonatite volcano, Oldoinyo Lengai (Tanzania), which
715 erupts natrocarbonatite. Other occurrences of natrocarbonatite are found only very
716 rarely as melt inclusions within igneous minerals from alkaline rocks^{162,165} and
717 kimberlites¹¹. The lack of natrocarbonatite from the rock record is often ascribed to its
718 extreme instability under atmospheric - and most geological - conditions¹⁶⁶. Rare earth
719 carbonatites (with >1 wt.% REE) also tend to be enriched in other incompatible trace
720 elements (e.g., U, Th, Nb, Ta) and are regarded to be products of fractional
721 crystallisation of parental carbonatite magma¹⁶⁷. This carbonatite class is of significant
722 economic importance as a source of the critical metals needed for many technological
723 applications that support modern societies¹⁶⁸.

724

725 Despite consensus of mantle origins, there are differing opinions on carbonatite
726 evolution. Some workers assert that carbonatites are primary magmas derived directly
727 by low degree melting of CO₂-rich mantle sources¹⁶⁹, whereas experimental work by
728 Watkinson and Wyllie¹⁷⁰ demonstrated that carbonate liquids could be formed as
729 residua of fractionation from carbonated peralkaline silicate magmas; this latter origin
730 would be consistent with a classification as 'carbothermal residua' of Mitchell¹⁶⁷.
731 Supporting a primary mantle origin are studies of mantle xenoliths of distinctive
732 petrological and geochemical character formed via metasomatism by carbonatitic
733 melt^{8,77,171}. Carbonatitic melt inclusions with diamond are further unequivocal evidence
734 of a mantle origin^{77,172}.

735

736 A third origin proposed for carbonatite genesis is via liquid immiscibility from evolving
737 CO₂-bearing alkaline silicate melt at crustal pressures⁷⁷. Support for this model comes
738 not only from experimental evidence and the common field association between
739 carbonatite and alkaline silicate magmatic rocks, but crucially from a growing number
740 of textural, petrological and geochemical studies of carbonatites^{165,173-175}. Given the
741 compelling evidence for primary mantle and immiscibility origins, it is likely that
742 carbonatite magmas may be formed in a range of geological environments from
743 shallow crustal down to lower mantle conditions.

744

745 Carbonatites and other mantle-derived CO₂-rich magmas, such as kimberlites, are
746 found across all continents, although over half are in Africa¹⁷⁶. They are most
747 commonly found within Precambrian cratons despite the fact that most are of
748 Phanerozoic age^{177,178}. These settings would be consistent with formation via low
749 degree (and hence, relatively low temperature) melting of fertile mantle sources, such
750 as thick mantle lithosphere beneath stable cratons. There tends to be an increasing
751 frequency of their formation towards younger ages, which is not easily explained as
752 an artefact of preservation¹⁷⁸, but rather may reflect more favourable conditions for
753 production of mantle-derived alkaline magmatism in the modern Earth. This would be
754 consistent with more effective recycling of crustal material into the mantle via modern-
755 style subduction processes, allowing production of the re-fertilised mantle domains
756 that are requisite sources of these magmas.

757

758 There are diverse views on the tectonic settings in which carbonatites and other CO₂-
759 bearing magmas form and are emplaced into the crust. Carbonatite magmatism is a
760 distinctive feature of recent igneous activity of the East African Rift, demonstrating a
761 link to intra-continental rifting, and potentially mantle plumes¹⁷⁹. Many older
762 carbonatite complexes have also been linked to continental rifting, mantle plumes, or
763 large igneous provinces¹⁸⁰⁻¹⁸². However, Woolley and Bailey¹⁷⁸ argue that ephemeral
764 mantle controls, such as mantle plumes do not account for the episodic and repeated
765 nature of carbonatitic (and kimberlitic) magmatism within restricted areas, sometimes
766 over billions of years. Instead, these authors argue that reactivation of lithospheric
767 scale structures or lineaments due to far-field plate reorganisation (e.g., due to rift
768 initiation or continental assembly¹⁸³), which allows for low degree melting of the fertile

769 cratonic mantle lithosphere to produce carbonatites or kimberlites, as well as efficient
770 tapping of the melts to the surface.

771

772 Carbonatites in oceanic settings have only been described from the hotspot volcanos
773 of Cape Verde and the Canary Islands^{184,185}. In these settings, the degree of mantle
774 melting is expected to be too high to produce carbonatites directly; rather the
775 carbonatites are interpreted to be products of fractionation and unmixing from alkali-
776 rich primitive basanite melts¹⁸⁶. In this case, the rarity of oceanic carbonatites may
777 reflect a lack of preservation and exposure, rather than unsuitable petrogenesis
778 conditions.

779

780 **6.10 Concluding remarks**

781

782 The existence of carbonate rich melts in the earth is likely limited in P-T- fO_2 space to
783 the crust, the uppermost part of the upper mantle including oceanic and continental
784 lithosphere, to the mantle wedge above subducting slabs, to locally strongly
785 metasomatised regions of the deep cratonic lithospheric mantle and asthenosphere,
786 and to local regions of the deep upper mantle, mantle transition zone and uppermost
787 lower mantle associated with deep subduction of carbonate-bearing oceanic
788 lithosphere. Much of the deep earth is too reduced for carbonate or carbonate-rich
789 melts to be stable and carbon will exist in reduced forms, such as diamond, methane
790 and other alkanes or volatile organic molecules, and Fe carbides.

791

792 Despite this, carbonate melts are of tremendous importance as agents of mass
793 transport and metasomatic enrichment in the earth's interior. They are also the primary
794 source of almost all commercially viable REE resources and may contain other critical
795 metals in extractable quantities as well. Although crustally emplaced carbonatites are
796 small in volume, they are likely to be much more abundant as broadly alkali-rich calcio-
797 dolomitic to dolomitic melts in the upper mantle and mantle transition zone, where they
798 contribute significantly to the carbon fluxes to the surface.

799

800 **Acknowledgements**

801 We gratefully thank the editorial team for this book, Beth Orcutt, Isabelle Daniel and
802 Raj Dasgupta for their encouragement and immense patience in the development of

803 this Chapter and for their expert editorial handling. We also thank Raj Dasgupta and
804 an anonymous reviewer for two constructive formal reviews.
805

806 **Figure Captions**

807

808 *Figure 1: Schematic cross section of a subduction zone (modified after⁷⁶) depicting*
809 *progressive slab devolatilisation during subduction and zones of the mantle wedge*
810 *containing carbonatitic and silicate-rich partial melts (green and orange fields,*
811 *respectively).*

812

813 *Figure 2. Summary of the experimentally determined solidus curves determined for*
814 *carbonated pelitic sediment and basaltic compositions. Solidus curves for carbonated*
815 *basalt are shown as solid coloured curves and are from: Hammouda⁹⁶, H03; Yaxley*
816 *and Brey¹⁴⁹, YB04; Dasgupta et al.⁹⁵, D04; Keshav and Gudfinnsson¹⁸⁷, KG10;*
817 *Kiseeva et al.¹², K13a,b; Thomson et al.¹³, T13. Labels are keyed to the compositions*
818 *listed in Table 1. Solidus curves for carbonated sediment are shown as dashed curves*
819 *and are from: Tsuno and Dasgupta⁹⁰, TD11; Grassi and Schmidt¹⁸⁸, GS11. Also*
820 *shown is the solidus of alkaline carbonatite (Litasov et al.¹⁰², L13). The mantle adiabat*
821 *is from Katsura et al.¹⁸⁹; Model geotherms at the top of a subducting slab are*
822 *extrapolations shown for examples of hot, warm and cold slabs⁶⁸.*

823

824 *Figure 3: The compositions of partial melts from carbonated natural basalt and*
825 *sediment from the studies of Hammouda⁹⁶, Dasgupta et al.⁹⁶, Kiseeva et al.¹²,*
826 *Thomson et al.¹³ and Grassi and Schmidt⁹¹. The generalized effect of increasing*
827 *pressure and temperature are also shown.*

828

829 *Figure 4: Highly schematic representation of a section through the earth's upper*
830 *mantle modified from Figure 2c of Foley and Fischer¹¹³, showing fO_2 as function of*
831 *depth. The dashed light blue contours are approximate contours of oxygen fugacity*
832 *variation in the cratonic lithosphere, based on studies of garnet peridotite xenoliths*
833 *(references in the text). The dashed yellow line is the graphite-diamond transition for*
834 *a typical cratonic geotherm (38 mWm^{-2}). The red line [1] represents the path of an*
835 *erupting kimberlite and the blue zone [2] near the base of the lithosphere represents*
836 *a local mantle volume metasomatised to higher fO_2 by asthenospheric melts derived*
837 *from the brown field labelled [1].*

838

839 *Figure 5. (a) Pressure-temperature plot showing the generation of carbonated silicate*
840 *melt in the Earth's upper mantle. A parcel of carbon-bearing mantle peridotite with*
841 *pods of eclogite upwells beneath ocean islands along an adiabat (bold arrow along*
842 *the dotted line). As it upwells, redox melting takes place when the mantle crosses over*
843 *from the stippled zone where the carbon is present in reduced form (either as graphite*
844 *or as diamond^{21,139}) to the overlying zone where carbon is present in its oxidized form*
845 *(as carbonates or as CO₂ vapor at pressures lower than 2 GPa³). At the redox front,*
846 *reduced carbon present in the eclogite or peridotite oxidizes to form trace to minor*
847 *amounts of carbonatitic melt (labelled 1 in the figure). The carbonatitic melt causes*
848 *flux-partial melting of eclogite and peridotite, because the carbonated solidus of*
849 *peridotite and eclogite are at a much lower temperature at the pressure range of the*
850 *upwelled parcel of mantle (labelled 2 in the figure). The flux partial melting of eclogite*
851 *and peridotite produce carbonated silicate melts in the upper mantle. The volatile-free*
852 *solidii of peridotite¹⁹⁰ and eclogite¹⁹¹, the carbonated solidi of peridotite^{33,143} and*
853 *eclogite¹⁴⁹, graphite-diamond transition¹⁹², and range of mantle potential temperatures*
854 *in the Earth's upper mantle (orange shaded area) from ridges¹⁹³ to plumes¹⁹⁴ are*
855 *plotted for reference. The broken curves for carbonated solidi are only applicable for*
856 *locally oxidized domains in the mantle where carbonates can exist at depths below*
857 *the redox-melting front. (b) Geodynamic scenarios involving carbonated eclogite and*
858 *peridotite in the source of ocean island volcanism in intraplate settings (modified from*
859 *a previous study¹⁵³); (i) This scenario is applicable for locally oxidized domains in the*
860 *mantle where deeper carbonatites generated by very low-degree partial melting of*
861 *carbonated peridotite and/or eclogite rise upwards and cause fluxed partial melting of*
862 *volatile-free eclogite at shallower depths in the upper mantle. The carbonated partial*
863 *melt of eclogite, a basanite or andesite (lower eclogite to carbonate ratio produces*
864 *basanite while a higher ratio produces andesite), reacts with subsolidus volatile-free*
865 *peridotite. The melt-rock reaction produces product melts that display similarity in*
866 *composition with ocean island basalts; (ii) Reduced carbon bearing eclogite upwells*
867 *and produces carbonated silicate partial melt of eclogite after crossing the redox-*
868 *melting front. The carbonated-silicate partial melt of eclogite reacts with the*
869 *surrounding subsolidus volatile-free peridotite, and a similar melt-rock reaction as*
870 *proposed in (i) takes place.*

871

872 *Figure 6: A simplified model for the extraction of carbonatitic/carbonated silicate melts*
873 *from the mantle based on Stagno et al.²⁸. If carbonates are present in the adiabatically*
874 *upwelling mantle beneath mid ocean ridges, they will lower the melting temperature of*
875 *the mantle rocks and melting will take place at ~ 300 km depth if the adiabat has a*
876 *potential temperature of 1400°C. Left hand side diagram shows solidus of peridotite*
877 *and eclogite is depressed by several hundred degree compared to volatile free solidus.*
878 *Centre panel shows the focussing of deeply derived carbonate melts (red triangle)*
879 *formed by redox melting at about 1.5 GPa lower pressures than the carbonate*
880 *peridotite solidus for oxidised mantle. Right hand panel shows estimated $Fe^{3+}/\Sigma Fe$ in*
881 *peridotite buffered at about 0.1 at depths below about 290 km, and buffered by FeNi*
882 *alloy ($\approx IW$) to higher values at greater depths.*
883

884 Table 1. Bulk compositions of anhydrous MORB and carbonated MORB used in
 885 melting studies

	G12	Y94	W99	H03	D04	K13a	K13b	T16
	All MORB	NAM-7	JB1	OTBC	SLEC1	GA1cc	Volgacc	ATCM1
SiO ₂	50.47	47.71	53.53	47.23	41.21	45.32	42.22	50.35
TiO ₂	1.68	1.71	1.44	-	2.16	1.34	1.43	1.33
Al ₂ O ₃	14.7	15.68	14.85	15.35	10.89	14.88	15.91	13.66
FeO	10.43	9.36	7.92	8.93	12.83	8.85	9.46	11.35
MnO	0.18	0.18	0.16	-	0.12	0.15	0.14	0.21
MgO	7.58	8.43	7.64	6.24	12.87	7.15	7.64	7.15
CaO	11.39	11.73	9.12	14.77	13.09	14.24	14.85	10.8
Na ₂ O	2.79	2.76	2.64	2.91	1.63	3.14	3.36	2.48
K ₂ O	0.16	0.23	1.31	0.02	0.11	0.4	0.42	0.06
P ₂ O ₅	0.18	0.02	-	-	-	0.14	0.15	0.1
CO ₂	-	-	-	4.43	5.0	4.4	4.4	2.52
Total	99.57	99.81	98.61	99.88	99.91	100.01	99.98	100
Ca#	0.38	0.38	0.38	0.48	0.32	0.46	0.45	0.36
Mg#	0.57	0.62	0.62	0.56	0.64	0.59	0.59	0.53

886 OTBC additionally contains 1200 ppm H₂O
 887 Ca number = Ca/[Ca+Mg+Fe]; Mg number = Mg/[Mg+Fe]
 888 G12 = Gale et al. (2012); Y94 = Yasuda et al. (1994); W99 = Wang and Takahashi (1999); D04 =
 889 Dasgupta et al. (2004); H03 = Hammouda (2003); K13 = Kiseeva et al. (2013); T16 = Thomson et al.
 891 (2016).
 892

893 ***Limits to knowledge and unknowns***

894

895 Key areas relating to carbonate or CO₂-bearing melts in the earth, in which current
896 knowledge is limited, include the solubility of CO₂ in hydrous fluids and partial melts
897 derived from subduction oceanic crust, particularly in the sub-arc environment. These
898 melts may have a critically important role in metasomatizing the mantle wedge and
899 fluxing melting, ultimately leading to arc volcanism and continental crust formation.
900 They are agents by which subducted carbon is recycled on relatively short time scales
901 of 10s of Ma from the subducted slab in the sub-arc environment (blueschist or eclogite
902 facies conditions), back to the atmosphere and hydrosphere. We cannot quantify
903 carbon fluxes in this relatively shallow part of the earth's deep carbon cycle, unless
904 we understand the magnitude of volatile fluxes from slab to arc volcanism. This will
905 require high pressure experimental studies as well as field studies of high grade,
906 carbonated metamorphic rocks in orogenic zones.

907

908 This in turn, bears on estimates of carbon fluxes via subduction into the deeper mantle,
909 ultimately to the mantle transition zone or lower mantle. These estimates currently
910 vary from 0-15 Mt/a⁵⁶. It appears likely that some carbon does escape relatively
911 shallow recycling during subduction to sub-arc conditions, based on studies of sub-
912 lithospheric diamonds and their inclusions. If so, it may then be transported as part of
913 oceanic lithosphere to the deeper mantle. However, it remains unclear how the oxygen
914 fugacity of the oceanic crustal components being subducted as part of the lithospheric
915 package varies along the prograde path. This will be a critical control on the ultimate
916 fate of carbon in oceanic crust. For example, as has been shown recently by Kiseeva
917 et al.¹² and Thomson et al.¹³, carbonate in mafic crust is unlikely to be subducted
918 beyond the mantle transition zone as it will melt to form carbonate liquids, which will
919 segregate from their source and undergo redox freezing on contact with reduced
920 peridotite wall rock¹³⁹. However, if carbonate is reduced to diamond on the prograde
921 path, melting will not occur and in those cases where slabs enter the lower mantle,
922 carbon will be likely also be transported beyond the mantle transition zone.

923

924 Finally, we currently lack understanding of aspects of the return cycle of carbon from
925 the deep upper mantle, mantle transition zone or lower mantle to the surface. In
926 particular, some sub-lithospheric diamonds originate from these very deep parts of the

927 upper and lower mantle, based on their mineral inclusions. However, it is unclear
928 exactly how and where the kimberlites formed, that host these diamonds and
929 transported them to the surface. Did they form at deep upper mantle, transition zone
930 or lower mantle pressures? Or were the sublithospheric diamonds first transported
931 from great depths in during mantle convection and then entrained in kimberlites formed
932 at depths just below the cratonic lithospheric mantle? This will require careful high
933 pressure experimental studies to deepen understanding of the role of COH-volatiles
934 in causing melting at depths in and around the transition zone.

935

936 **Chapter questions for the classroom**

937

938 1. Describe the different forms in which carbon is believed to exist in the Earth's
939 mantle. In which parts of the mantle are these different carbon-bearing species
940 located and what is the evidence for their presence?

941

942 2. Explain how pressure, temperature and oxygen fugacity in the Earth's mantle
943 influence the species present in different parts of the mantle (lower mantle,
944 mantle transition zone, upper mantle) and different tectonic settings.

945

946 3. What are some of the reasons that carbonate melts inferred to exist in parts of
947 the sub-continental lithosphere are considered to be highly effective
948 metasomatic agents?

949

950 4. Carbonate is a wide-spread component of oceanic crust hydrothermally altered
951 near mid-ocean ridges. When transported by plate tectonics to subduction
952 zones, this carbonate may be recycled back into the mantle. Describe some of
953 the processes which may influence the fate and redistribution of this subducted
954 carbon in the fore-arc, sub-arc and deeper environments.

955

956 5. How does oxygen fugacity vary within the Earth's mantle? What are the major
957 controls on this variation and why is it important in understanding the Earth's
958 deep carbon cycle?

959

960 6. Sub-lithospheric diamonds are believed to have formed at depths greater than
961 the lithosphere-asthenosphere boundary, i.e. they did not form within the
962 cratonic mantle lithosphere like the majority of kimberlite-bourne diamonds.
963 From where are they derived and how are they likely to have formed? What is
964 the evidence?

965

966 7. The only currently active carbonatite volcano on Earth is Oldoinyo Lengai, in
967 Tanzania. How are the carbonatites erupted by this volcano different to all other
968 known crustally emplaced carbonatites? Do some literature research to
969 understand some of the hypotheses for the formation of Oldoinyo Lengai's
970 lavas, and possible reasons that it is so anomalous relative to other older
971 carbonatites.

972

973 8. What are the likely reasons for the absence of crustally emplaced carbonatite
974 melts in subduction zones?

975

976 9. Describe ways in which CO₂-rich silicate melts can form in the Earth's upper
977 mantle. In what sorts of tectonic settings are these melts likely to erupt?

978

979 10. Draw a cross-section of the Earth, showing the main tectonic settings (e.g. mid-
980 ocean ridge, subduction zone, intraplate volcanic setting, continental and
981 cratonic setting etc) and illustrate the locations of major carbon reservoirs and
982 the nature of the carbon-bearing species that may be present in each. Discuss
983 processes by which carbon may move between these reservoirs.

984

985

986 **References**

- 987
- 988 1 Dawson, J. B. Sodium Carbonate Lavas from Oldoinyo Lengai, Tanganyika.
989 *Nature* **195**, 1075, (1962).
- 990 2 Wyllie, P. J., Baker, M. B. & White, B. S. Experimental boundaries for the
991 origin and evolution of carbonatites. *Lithos* **26**, 3-19, (1990).
- 992 3 Wallace, M. E. & Green, D. H. An Experimental-Determination of Primary
993 Carbonatite Magma Composition. *Nature* **335**, 343-346 (1988).
- 994 4 Yaxley, G. & Brey, G. Phase relations of carbonate-bearing eclogite
995 assemblages from 2.5 to 5.5 GPa: implications for petrogenesis of
996 carbonatites. *Contrib Mineral Petrol* **146**, 606-619, (2004).
- 997 5 Dasgupta, R. & Hirschmann, M. M. Melting in the Earth's deep upper mantle
998 caused by carbon dioxide. *Nature* **440**, 659-662 (2006).
- 999 6 Dasgupta, R. & Hirschmann, M. M. The deep carbon cycle and melting in
1000 Earth's interior. *Earth Planet Sci Lett* **298**, 1-13 (2010).
- 1001 7 Yaxley, G., Crawford, A. & Green, D. Evidence for carbonatite metasomatism
1002 in spinel peridotite xenoliths from western Victoria, Australia. *Earth Planet Sci*
1003 *Lett* **107**, 305-317 (1991).
- 1004 8 Yaxley, G., Green, D. & Kamenetsky, V. Carbonatite metasomatism in the
1005 southeastern Australian lithosphere. *J Petrol* **39**, 1917-1930 (1998).
- 1006 9 Rudnick, R. L., McDonough, W. F. & Chappell, B. W. Carbonatite
1007 Metasomatism in the Northern Tanzanian Mantle - Petrographic and
1008 Geochemical Characteristics. *Earth Planet Sci Lett* **114**, 463-475 (1993).
- 1009 10 Weiss, Y., McNeill, J., Pearson, D. G., Nowell, G. M. & Ottley, C. J. Highly
1010 saline fluids from a subducting slab as the source for fluid-rich diamonds.
1011 *Nature* **524**, 339-342, (2015).
- 1012 11 Golovin, A. V., Sharygin, I. S., Kamenetsky, V. S., Korsakov, A. V. & Yaxley,
1013 G. M. Alkali-carbonate melts from the base of cratonic lithospheric mantle:
1014 Links to kimberlites. *Chem Geol* **483**, 261-274, (2018).
- 1015 12 Kiseeva, E. S., Litasov, K. D., Yaxley, G. M., Ohtani, E. & Kamenetsky, V. S.
1016 Melting and Phase Relations of Carbonated Eclogite at 9-21 GPa and the
1017 Petrogenesis of Alkali-Rich Melts in the Deep Mantle. *J Petrol* **54**, 1555-1583,
1018 (2013).
- 1019 13 Thomson, A. R., Walter, M. J., Kohn, S. C. & Brooker, R. A. Slab melting as a
1020 barrier to deep carbon subduction. *Nature* **529**, 76-79, (2016).
- 1021 14 Litasov, K. & Ohtani, E. Solidus of carbonate eclogite in the system CaO-
1022 Al₂O₃-MgO-SiO₂-Na₂O-CO₂ to 32 GPa and carbonatite liquid un the deep
1023 mantle. *Earth Planet Sci Lett* **295**, 115-126 (2010).
- 1024 15 Kaminsky, F. Mineralogy of the lower mantle: A review of 'super-deep' mineral
1025 inclusions in diamond. *Earth-Sci Rev* **110**, 127-147, (2012).
- 1026 16 Hunter, R. H. & Mckenzie, D. The Equilibrium Geometry of Carbonate Melts in
1027 Rocks of Mantle Composition. *Earth Planet Sci Lett* **92**, 347-356 (1989).
- 1028 17 Hammouda, T. & Laporte, D. Ultrafast mantle impregnation by carbonatite
1029 melts. *Geology* **28**, 283-285, (2000).
- 1030 18 Shatskiy, A. *et al.* Silicate diffusion in alkali-carbonatite and hydrous melts at
1031 16.5 and 24GPa: Implication for the melt transport by dissolution–precipitation
1032 in the transition zone and uppermost lower mantle. *Phys Earth Planet Int* **225**,
1033 1-11, (2013).
- 1034 19 Taylor, W. R. & Green, D. H. The petrogenic role of methane: Effect on
1035 liquidus phase relations and the solubility mechanism of reduced C-H

- 1036 volatiles. *The Geochemical Society Special Publication No. 1*, 121-137
 1037 (1987).
- 1038 20 Luth, R. W. Diamonds, Eclogites, and the Oxidation-State of the Earths
 1039 Mantle. *Science* **261**, 66-68 (1993).
- 1040 21 Stagno, V., Ojwang, D. O., McCammon, C. A. & Frost, D. J. The oxidation
 1041 state of the mantle and the extraction of carbon from Earth's interior. *Nature*
 1042 **493**, 84-88, (2013).
- 1043 22 Kennedy, C. S. & Kennedy, G. C. The equilibrium boundary between graphite
 1044 and diamond. *J Geophys Res* **81**, 2467-2470 (1976).
- 1045 23 Yaxley, G. M., Berry, A. J., Rosenthal, A., Woodland, A. B. & Paterson, D.
 1046 Redox preconditioning deep cratonic lithosphere for kimberlite genesis -
 1047 evidence from the central Slave Craton. *Nature Scientific Reports* **7**, 30
 1048 (2017).
- 1049 24 Kiseeva, E. S. *et al.* Oxidized iron in garnets from the mantle transition zone.
 1050 *Nature Geoscience*, (2018).
- 1051 25 Cottrell, E. & Kelley, K. A. The oxidation state of Fe in MORB glasses and the
 1052 oxygen fugacity of the upper mantle. *Earth Planet Sci Lett* **305**, 270-282,
 1053 (2011).
- 1054 26 Berry, A. J., Stewart, G. A., O'Neill, H. S. C., Mallmann, G. & Mosselmans, J.
 1055 F. W. A re-assessment of the oxidation state of iron in MORB glasses. *Earth*
 1056 *Planet Sci Lett* **483**, 114-123, (2018).
- 1057 27 Gudmundsson, G. & Wood, B. J. Experimental Tests of Garnet Peridotite
 1058 Oxygen Barometry. *Contrib Mineral Petrol* **119**, 56-67 (1995).
- 1059 28 Stagno, V., Frost, D. J., McCammon, C. A., Mohseni, H. & Fei, Y. The oxygen
 1060 fugacity at which graphite or diamond forms from carbonate-bearing melts in
 1061 eclogitic rocks. *Contrib Mineral Petrol* **169**, 16, (2015).
- 1062 29 Stagno, V. & Frost, D. J. Carbon speciation in the asthenosphere:
 1063 Experimental measurements of the redox conditions at which carbonate-
 1064 bearing melts coexist with graphite or diamond in peridotite assemblages.
 1065 *Earth Planet Sci Lett* **300**, 72-84 (2010).
- 1066 30 Falloon, T. J. & Green, D. H. The solidus of carbonated, fertile peridotite.
 1067 *Earth Planet Sci Lett* **94**, 364-370, (1989).
- 1068 31 Falloon, T. J. & Green, D. H. Solidus of Carbonated Fertile Peridotite under
 1069 Fluid-Saturated Conditions. *Geology* **18**, 195-199 (1990).
- 1070 32 Dasgupta, R. & Hirschmann, M. M. Effect of variable carbonate concentration
 1071 on the solidus of mantle peridotite. *Am Mineral* **92**, 370-379 (2007).
- 1072 33 Dasgupta, R., Hirschmann, M. M. & Smith, N. D. Partial Melting Experiments
 1073 of Peridotite + CO₂ at 3 GPa and Genesis of Alkalic Ocean Island Basalts *J.*
 1074 *Petrology* **48**, 2093-2124 (2007).
- 1075 34 Dasgupta, R., Hirschmann, M. M. & Smith, N. D. Water follows carbon: CO₂
 1076 incites deep silicate melting and dehydration beneath mid-ocean ridges.
 1077 *Geology* **35**, 135-138 (2007).
- 1078 35 Dasgupta, R., Stalker, K., Withers, A. C. & Hirschmann, M. M. The transition
 1079 from carbonate-rich to silicate-rich melts in eclogite: Partial melting
 1080 experiments of carbonated eclogite at 3 GPa. *Lithos* **73**, S23-S23 (2004).
- 1081 36 Lee, W. J. & Wyllie, P. J. Petrogenesis of carbonatite magmas from mantle to
 1082 crust, constrained by the system CaO-(MgO+FeO*)(Na₂O+K₂O)-
 1083 (SiO₂+Al₂O₃+TiO₂)-CO₂. *J Petrol* **39**, 495-517.
- 1084 37 Ryabchikov, I. D., Edgar, A. D. & Wyllie, P. J. Partial melting in the system
 1085 carbonate phosphate peridotite at 30 kbar. *Geokhimiya*, 163-168 (1991).

- 1086 38 White, B. S. & Wyllie, P. J. Solidus reactions in synthetic lherzolite-H₂O-CO₂
1087 from 20-30kbar, with applications to melting and metasomatism. *J Volcanol*
1088 *Geoth Res* **50**, 117-130, (1992).
- 1089 39 Wyllie, P. J. Peridotite-CO₂-H₂O and carbonatitic liquids in upper
1090 asthenosphere. *Nature* **266**, 45-47, (1977).
- 1091 40 Wyllie, P. J. Mantle Fluid Compositions Buffered in Peridotite-CO₂-H₂O by
1092 Carbonates, Amphibole, and Phlogopite. *J Geol* **86**, 687-713 (1978).
- 1093 41 Wyllie, P. J. Fusion of Peridotite-H₂O-CO₂ in System Peridotite-H-C-O at
1094 Upper Mantle Pressures. *Eos Trans American Geophysical Union* **59**, 398-
1095 398 (1978).
- 1096 42 Newton, R. C. & Sharp, W. E. Stability of forsterite + CO₂ and its bearing on
1097 the role of CO₂ in the mantle. *Earth Planet Sci Lett* **26**, 239-244, (1975).
- 1098 43 Haselton, H. T., Sharp, W. E. & Newton, R. C. CO₂ fugacity at high
1099 temperatures and pressures from experimental decarbonation reactions.
1100 *Geophys Res Lett* **5**, 753 (1978).
- 1101 44 Egger, D. H., Kushiro, J. & Holloway, J. R. Free energies of decarbonation
1102 reactions at mantle pressures, I. Stability of the assemblage forsterite-
1103 enstatite-magnesite in the system MgO-SiO₂-CO₂-H₂O to 60 kbar. *Am Mineral*
1104 **64**, 288 (1979).
- 1105 45 Johannes, W. An experimental investigation of the system MgO-SiO₂-H₂O-
1106 CO₂. *Am J Sci* **267**, 1083 (1969).
- 1107 46 Wyllie, P. J. Magmass and volatile components. *Am Mineral* **64**, 469-500
1108 (1979).
- 1109 47 Egger, D. H. The effect of CO₂ on partial melting of peridotite in the system
1110 Na₂O-CaO-Al₂O₃-MgO-SiO₂-CO₂ to 35 kbar, with an analysis of melting in a
1111 peridotite-H₂O-CO₂ system. *Am J Sci* **278**, 305 (1978).
- 1112 48 Kushiro, I. Carbonate-silicate reactions at high pressures and possible
1113 presence of dolomite and magnesite in the upper mantle. *Earth Planet Sci*
1114 *Lett* **28**, 116-120,(1975).
- 1115 49 Brey, G. *et al.* Pyroxene-carbonate reactions in the upper mantle. *Earth*
1116 *Planet Sci Lett* **62**, 63-74, (1983).
- 1117 50 Yaxley, G. M., Crawford, A. J. & Green, D. H. Evidence for Carbonatite
1118 Metasomatism in Spinel Peridotite Xenoliths from Western Victoria, Australia.
1119 *Earth Planet Sci Lett* **107**, 305-317 (1991).
- 1120 51 Rudnick, R. L., McDonough, W. F. & Chappell, B. W. Carbonatite
1121 metasomatism in the northern Tanzanian mantle: Petrographic and
1122 geochemical characteristics. *Earth Planet Sci Lett* **114**, 463-475, (1993).
- 1123 52 Dalton, J. A. & Wood, B. J. The Compositions of Primary Carbonate Melts and
1124 Their Evolution through Wallrock Reaction in the Mantle. *Earth Planet Sci Lett*
1125 **119**, 511-525 (1993).
- 1126 53 Foley, S. F. *et al.* The composition of near-solidus melts of peridotite in the
1127 presence of CO₂ and H₂O between 40 and 60 kbar. *Lithos* **112**, 274-283
1128 (2009).
- 1129 54 Marty, B. The origins and concentrations of water, carbon, nitrogen and noble
1130 gases on Earth. *Earth Planet Sci Lett* **313-314**, 56-66, (2012).
- 1131 55 Sleep, N. H. & Zahnle, K. Carbon dioxide cycling and implications for climate
1132 on ancient Earth. *Journal of Geophysical Research: Planets* **106**, 1373-1399.
- 1133 56 Kelemen, P. B. & Manning, C. E. Reevaluating carbon fluxes in subduction
1134 zones, what goes down, mostly comes up. *Proceedings of the National*
1135 *Academy of Sciences* **112**, E3997-E4006, (2015).

- 1136 57 Plank, T. & Langmuir, C. H. The chemical composition of subducting sediment
1137 and its consequences for the crust and mantle. *Chem Geol* **145**, 325-394
1138 (1998).
- 1139 58 Plank, T. The chemical composition of subducting sediments. *Treatise on
1140 Geochemistry* **4**, 607-629 (2014).
- 1141 59 Alt, J. C. & Teagle, D. A. H. The uptake of carbon during alteration of ocean
1142 crust. *Geochim Cosmochim Acta* **63**, 1527-1535 (1999).
- 1143 60 Connolly, J. A. D. Computation of phase equilibria by linear programming; A
1144 tool for geodynamic modelling and its application to subduction zone
1145 decarbonation. *Earth Planet Sci Lett* **236**, 524-541 (2005).
- 1146 61 Connolly, J. A. D. Computation of phase equilibria by linear programming: A
1147 tool for geodynamic modeling and its application to subduction zone
1148 decarbonation. *Earth Planet Sci Lett* **236**, 524-541, (2005).
- 1149 62 Manning, C. E., Shock, E. L. & Sverjensky, D. A. The chemistry of carbon in
1150 aqueous fluids at crustal and upper-mantle conditions: experimental and
1151 theoretical constraints. *Reviews in Mineralogy and Geochemistry* **75**, 109-148
1152 (2013).
- 1153 63 Ague, J. J. & Nicolescu, S. Carbon dioxide released from subduction zones by
1154 fluid-mediated reactions. *Nature Geoscience* **7**, 355, (2014).
- 1155 64 Piccoli, F. *et al.* Carbonation by fluid–rock interactions at high-pressure
1156 conditions: Implications for carbon cycling in subduction zones. *Earth Planet
1157 Sci Lett* **445**, 146-159, (2016).
- 1158 65 Spandler, C., Hermann, J., Faure, K., Mavrogenes, J. A. & Arculus, R. J. The
1159 importance of talc and chlorite “hybrid” rocks for volatile recycling through
1160 subduction zones; evidence from the high-pressure subduction mélange of
1161 New Caledonia. *Contrib Mineral Petrol* **155**, 181-198, (2008).
- 1162 66 Scambelluri, M. *et al.* Carbonation of subduction-zone serpentinite (high-
1163 pressure ophicarbonates; Ligurian Western Alps) and implications for the deep
1164 carbon cycling. *Earth Planet Sci Lett* **441**, 155-166, (2016).
- 1165 67 Sieber, M. J., Hermann, J. & Yaxley, G. M. An experimental investigation of
1166 C–O–H fluid-driven carbonation of serpentinites under forearc conditions.
1167 *Earth Planet Sci Lett* **496**, 178-188, (2018).
- 1168 68 Syracuse, E. M., van Keken, P. E. & Abers, G. A. The global range of
1169 subduction zone thermal models. *Phys Earth Planet In* **183**, 73-90, (2010).
- 1170 69 Frezzotti, M. L., Selverstone, J., Sharp, Z. D. & Compagnoni, R. Carbonate
1171 dissolution during subduction revealed by diamond-bearing rocks from the
1172 Alps. *Nature Geoscience* **4**, 703, (2011).
- 1173 70 Schmidt, M. W. Melting of pelitic sediments at subarc depths: 2. Melt
1174 chemistry, viscosities and a parameterization of melt composition. *Chem Geol*
1175 **404**, 168-182, (2015).
- 1176 71 Korsakov, A. V. & Hermann, J. Silicate and carbonate melt inclusions
1177 associated with diamonds in deeply subducted carbonate rocks. *Earth Planet
1178 Sci Lett* **241**, 104-118 (2006).
- 1179 72 Poli, S. Carbon mobilized at shallow depths in subduction zones by
1180 carbonatitic liquids. *Nature Geoscience* **8**, 633, (2015).
- 1181 73 Marschall, H. R. & Schumacher, J. C. Arc magmas sourced from melange
1182 diapirs in subduction zones. *Nature Geosci* **5**, 862-867, (2012).
- 1183 74 Tumati, S., Fumagalli, P., Tiraboschi, C. & Poli, S. An Experimental Study on
1184 COH-bearing Peridotite up to 3.2 GPa and Implications for Crust–Mantle
1185 Recycling. *J Petrol* **54**, 453-479, (2013).

- 1186 75 Smith, C. B. *et al.* Diamonds from Dachine, French Guiana: A unique record
1187 of early Proterozoic subduction. *Lithos* **265**, 82-95, (2016).
- 1188 76 Green, D. H. Experimental petrology of peridotites, including effects of water
1189 and carbon on melting in the Earth's upper mantle. *Phys Chem Miner* **42**, 95-
1190 122, (2015).
- 1191 77 Jones, A. P., Genge, M. & Carmody, L. in *Reviews in Mineralogy and*
1192 *Geochemistry* Vol. 75 289-322 (2013).
- 1193 78 Saha, S., Dasgupta, R. & Tsuno, K. High pressure phase relations of a
1194 depleted peridotite fluxed by CO₂-H₂O-bearing siliceous melts and the origin
1195 of Mid-Lithospheric Discontinuity. *Geochemistry, Geophysics, Geosystems*
1196 **19**, 595-620, (2018).
- 1197 79 Gorman, P. J., Kerrick, D. M. & Connolly, J. A. D. Modeling open system
1198 metamorphic decarbonation of subducting slabs. *Geochem Geophys Geosy* **7**,
1199 - (2006).
- 1200 80 Molina, J. F. & Poli, S. Carbonate stability and fluid composition in subducted
1201 oceanic crust: an experimental study on H₂O-CO₂-bearing basalts. *Earth*
1202 *Planet Sci Lett* **176**, 295-310 (2000).
- 1203 81 Kelley, K. A. & Cottrell, E. The influence of magmatic differentiation on the
1204 oxidation state of Fe in a basaltic arc magma. *Earth Planet Sci Lett* **329-330**,
1205 109-121 (2012).
- 1206 82 Brenker, F. E. *et al.* Carbonates from the lower part of transition zone or even
1207 the lower mantle. *Earth Planet Sci Lett* **260**, 1-9 (2007).
- 1208 83 Bulanova, G. P. *et al.* Mineral inclusions in sublithospheric diamonds from
1209 Collier 4 kimberlite pipe, Juina, Brazil: subducted protoliths, carbonated melts
1210 and primary kimberlite magmatism. *Contrib Mineral Petrol* **160**, 489-510,
1211 (2010).
- 1212 84 Thomson, A. R. *et al.* Origin of sub-lithospheric diamonds from the Juina-5
1213 kimberlite (Brazil): constraints from carbon isotopes and inclusion
1214 compositions. *Contrib Mineral Petrol* **168**, 1081 (2014).
- 1215 85 Zedgenizov, D. A., Kagi, H., Shatsky, V. S. & Ragozin, A. L. Local variations
1216 of carbon isotope composition in diamonds from Sao-Luis (Brazil): evidence
1217 for heterogenous carbon reservoir in sublithospheric mantle. *Chem Geol* **363**,
1218 114-124 (2010).
- 1219 86 Thomson, A. R. *et al.* Trace element composition of silicate inclusions in sub-
1220 lithospheric diamonds from the Juina-5 kimberlite: Evidence for diamond
1221 growth from slab melts. *Lithos* **265**, 108-124, (2016).
- 1222 87 Walter, M. J. *et al.* Primary carbonatite melt from deeply subducted oceanic
1223 crust. *Nature* **454**, 622, (2008).
- 1224 88 Burnham, A. D. *et al.* Stable isotope evidence for crustal recycling as
1225 recorded by superdeep diamonds. *Earth Planet Sci Lett* **432**, 374-380, (2015).
- 1226 89 Ickert, R. B., Stachel, T., Stern, R. A. & Harris, J. W. Diamond from recycled
1227 crustal carbon documented by coupled $\delta^{18}\text{O}$ - $\delta^{13}\text{C}$ measurements of
1228 diamonds and their inclusions. *Earth Planet Sci Lett* **364**, 85-97, (2013).
- 1229 90 Tsuno, K. & Dasgupta, R. Melting phase relation of nominally anhydrous,
1230 carbonated pelitic-eclogite at 2.5–3.0 GPa and deep cycling of sedimentary
1231 carbon. *Contrib Mineral Petrol* **161**, 743-763 (2011).
- 1232 91 Grassi, D. & Schmidt, M. W. Melting of carbonated pelites at 8-13 GPa:
1233 Generating K-rich carbonatites for mantle metasomatism. *Contrib Mineral*
1234 *Petrol* **162**, 169-191 (2011).

- 1235 92 Mann, U. & Schmidt, M. W. Melting of pelitic sediments at subarc depths: 1.
1236 Flux vs. fluid-absent melting and a parameterization of melt productivity.
1237 *Chem Geol* **404**, 150-167, (2015).
- 1238 93 Keshav, S. & Gudfinnsson Gudmundur, H. Experimentally dictated stability of
1239 carbonated oceanic crust to moderately great depths in the Earth: Results
1240 from the solidus determination in the system CaO-MgO-Al₂O₃-SiO₂-CO₂.
1241 *Journal of Geophysical Research: Solid Earth* **115**, (2010).
- 1242 94 Litasov, K. & Ohtani, E. The solidus of carbonated eclogite in the system
1243 CaO-Al₂O₃-MgO-SiO₂-Na₂O-CO₂ to 32GPa and carbonatite liquid in the
1244 deep mantle. *Earth Planet Sci Lett* **295**, 115-126, (2010).
- 1245 95 Dasgupta, R., Hirschmann, M. M. & Withers, A. C. Deep global cycling of
1246 carbon constrained by the solidus of anhydrous, carbonated eclogite under
1247 upper mantle conditions. *Earth Planet Sci Lett* **227**, 73-85 (2004).
- 1248 96 Hammouda, T. High-pressure melting of carbonated eclogite and
1249 experimental constraints on carbon recycling and storage in the mantle. *Earth
1250 Planet Sci Lett* **214**, 357-368 (2003).
- 1251 97 Kiseeva, E. S. *et al.* An Experimental Study of Carbonated Eclogite at 3.5-5.5
1252 GPa - Implications for Silicate and Carbonate Metasomatism in the Cratonic
1253 Mantle. *J Petrol* **53**, 727-759, (2012).
- 1254 98 Yaxley, G. M. & Green, D. H. Experimental demonstration of refractory
1255 carbonate-bearing eclogite and siliceous melt in the subduction regime. *Earth
1256 Planet Sci Lett* **128**, 313-325 (1994).
- 1257 99 Dasgupta, R., Hirschmann, M. M. & Dellas, N. The effect of bulk composition
1258 on the solidus of carbonated eclogite from partial melting experiments at 3
1259 GPa. *Contrib Mineral Petrol* **149**, 288-305 (2005).
- 1260 100 Gerbode, C. & Dasgupta, R. Carbonate-fluxed Melting of MORB-like
1261 Pyroxenite at 2-9 GPa and Genesis of HIMU Ocean Island Basalts. *J Petrol*
1262 **51**, 2067-2088, (2010).
- 1263 101 Dasgupta, R., Hirschmann, M. M. & Stalker, K. Immiscible transition from
1264 carbonate-rich to silicate-rich melts in the 3 GPa melting interval of eclogite +
1265 CO₂ and genesis of silica-undersaturated ocean island lavas. *J Petrol* **47**,
1266 647-671 (2006).
- 1267 102 Litasov, K. D., Shatskiy, A., Ohtani, E. & Yaxley, G. M. Solidus of alkaline
1268 carbonatite in the deep mantle. *Geology* **41**, 79-82 (2013).
- 1269 103 Gudfinnsson, G. H. & Presnall, D. C. Continuous gradations among primary
1270 carbonatitic, kimberlitic, melilititic, basaltic, picritic, and komatiitic melts in
1271 equilibrium with garnet lherzolite at 3-8GPa. *J Petrol* **46**, 1645-1659 (2005).
- 1272 104 Tappe, S., Foley, S. F., Jenner, G. A. & Kjarsgaard, B. A. Integrating
1273 ultramafic lamprophyres into the IUGS classification of igneous rocks:
1274 Rationale and implications. *J Petrol* **46**, 1893-1900 (2005).
- 1275 105 Tappe, S. *et al.* Between carbonatite and lamproite - Diamondiferous Torngat
1276 ultramafic lamprophyres formed by carbonate-fluxed melting of cratonic
1277 MARID-type metasomes. *Geochim Cosmochim Acta* **72**, 3258-3286 (2008).
- 1278 106 Sparks, R. S. J. Kimberlite Volcanism. *Annual Rev Earth Planet Sci* **41**, 497-
1279 528.
- 1280 107 Mitchell, R. H. *Kimberlites, orangeites, and related rocks*. (Plenum Press,
1281 1995).
- 1282 108 Becker, M. & Le Roex, A. P. Geochemistry of South African on- and off-
1283 craton, Group I and Group II kimberlites: Petrogenesis and source region
1284 evolution. *J Petrol* **47**, 673-703 (2006).

- 1285 109 Mitchell, R. H. Kimberlites and Lamproites - Primary Sources of Diamond.
1286 *Geosci Can* **18**, 1-16 (1991).
- 1287 110 Nowell, G. M. *et al.* Hf isotope systematics of kimberlites and their
1288 megacrysts: New constraints on their source regions. *J Petrol* **45**, 1583-1612
1289 (2004).
- 1290 111 Yaxley, G. M. *et al.* The discovery of kimberlites in Antarctica extends the vast
1291 Gondwanan Cretaceous province. *Nat. Commun.* **4** (2013).
- 1292 112 Novella, D. & Frost, D. J. The Composition of Hydrous Partial Melts of Garnet
1293 Peridotite at 6 GPa: Implications for the Origin of Group II Kimberlites. *J Petrol*
1294 **55**, 2097-2124, (2014).
- 1295 113 Foley, S. F. & Fischer, T. P. An essential role for continental rifts and
1296 lithosphere in the deep carbon cycle. *Nature Geoscience*, (2017).
- 1297 114 Patterson, M., Francis, D. & McCandless, T. Kimberlites: Magmas or
1298 mixtures? *Lithos* **112**, 191-200 (2009).
- 1299 115 Kamenetsky, M. B. *et al.* Kimberlite melts rich in alkali chlorides and
1300 carbonates: A potent metasomatic agent in the mantle. *Geology* **32**, 845-848
1301 (2004).
- 1302 116 Kamenetsky, V. S. *et al.* Olivine in the Udachnaya-East kimberlite (Yakutia,
1303 Russia): types, compositions and origins. *J Petrol* (2007).
- 1304 117 Russell, J. K., Porritt, L. A., Lavalley, Y. & Dingwell, D. B. Kimberlite ascent by
1305 assimilation-fuelled buoyancy. *Nature* **481**, 352-356, (2012).
- 1306 118 Girnis, A. V., Brey, G. P. & Ryabchikov, I. D. Origin of Group 1A kimberlites:
1307 Fluid-saturated melting experiments at 45-55 kbar. *Earth Planet Sci Lett* **134**,
1308 (1995).
- 1309 119 Girnis, A. V., Bulatov, V. K. & Brey, G. P. Formation of primary kimberlite
1310 melts - Constraints from experiments at 6-12GPa and variable CO₂/H₂O.
1311 *Lithos* **127**, 401-413, (2011).
- 1312 120 Nell, J. & Wood, B. J. High-temperature electrical measurements and
1313 thermodynamic properties of Fe₃O₄-FeCr₂O₄-MgCr₂O₄-FeAl₂O₄ spinels.
1314 *American Mineral* **76**, 405-426 (1991).
- 1315 121 Ballhaus, C., Berry, R. F. & Green, D. H. High-Pressure Experimental
1316 Calibration of the Olivine-Ortho-Pyroxene-Spinel Oxygen Geobarometer -
1317 Implications for the Oxidation-State of the Upper Mantle. *Contrib Mineral*
1318 *Petrol* **107**, 27-40 (1991).
- 1319 122 O'Neill, H. S. C. & Wall, V. J. The Olivine—Orthopyroxene—Spinel Oxygen
1320 Geobarometer, the Nickel Precipitation Curve, and the Oxygen Fugacity of the
1321 Earth's Upper Mantle. *J Petrol* **28**, 1169-1191 (1987).
- 1322 123 Woodland, A. B. & Koch, M. Variation in oxygen fugacity with depth in the
1323 upper mantle beneath the Kaapvaal craton, Southern Africa. *Earth Planet Sci*
1324 *Lett* **214**, 295-310 (2003).
- 1325 124 Yaxley, G. M., Berry, A. J., Kamenetsky, V. S., Woodland, A. B. & Golovin, A.
1326 V. An oxygen fugacity profile through the Siberian Craton—Fe K-edge XANES
1327 determinations of Fe³⁺/Σ Fe in garnets in peridotite xenoliths from the
1328 Udachnaya East kimberlite. *Lithos* **140**, 142-151 (2012).
- 1329 125 Frost, D. J. & McCammon, C. A. The redox state of Earth's mantle. *Annual*
1330 *Rev Earth Planet Sci* **36**, 389-420, (2008).
- 1331 126 Rohrbach, A., Ghosh, S., Schmidt, M. W., Wijbrans, C. H. & Klemme, S. The
1332 stability of Fe–Ni carbides in the Earth's mantle: Evidence for a low Fe–Ni–C
1333 melt fraction in the deep mantle. *Earth Planet Sci Lett* **388**, 211-221, (2014).

- 1334 127 Tsuno, K. & Dasgupta, R. Fe–Ni–Cu–C–S phase relations at high pressures
1335 and temperatures – The role of sulfur in carbon storage and diamond stability
1336 at mid- to deep-upper mantle. *Earth Planet Sci Lett* **412**, 132-142, (2015).
- 1337 128 Yaxley, G. M., Berry, A. J., Kamenetsky, V. S., Woodland, A. B. & Golovin, A.
1338 V. An oxygen fugacity profile through the Siberian Craton; Fe K-edge XANES
1339 determinations of Fe³⁺/ΣFe in garnets in peridotite xenoliths from the
1340 Udachnaya East kimberlite. *Lithos* **140-141**, 142-151 (2012).
- 1341 129 Foley, S. F. Rejuvenation and erosion of the cratonic lithosphere. *Nature*
1342 *Geoscience* **1**, 503-510 (2008).
- 1343 130 Coltorti, M., Beccaluva, L., Bonadiman, C., Salvini, L. & Siena, F. Glasses in
1344 mantle xenoliths as geochemical indicators of metasomatic agents. *Earth*
1345 *Planet Sci Lett* **183**, 303-320 (2000).
- 1346 131 Delpech, G. *et al.* Feldspar from carbonate-rich silicate metasomatism in the
1347 shallow oceanic mantle under Kerguelen Islands (South Indian Ocean). *Lithos*
1348 **75**, 209-237 (2004).
- 1349 132 Misra, K. C., Anand, M., Taylor, L. A. & Sobolev, N. V. Multi-stage
1350 metasomatism of diamondiferous eclogite xenoliths from the Udachnaya
1351 kimberlite pipe, Yakutia, Siberia. *Contrib Mineral Petrol* **146**, 696-714 (2004).
- 1352 133 Taylor, W. R. & Green, D. H. Measurement of Reduced Peridotite-C-O-H
1353 Solidus and Implications for Redox Melting of the Mantle. *Nature* **332**, 349-
1354 352 (1988).
- 1355 134 Litasov, K. D., Shatskiy, A. & Ohtani, E. Melting and subsolidus phase
1356 relations in peridotite and eclogite systems with reduced COH fluid at 3–16
1357 GPa. *Earth Planet Sci Lett* **391**, 87-99, (2014).
- 1358 135 Eguchi, J. & Dasgupta, R. Redox state of the convective mantle from CO₂-
1359 trace element systematics of oceanic basalts. *Geochemical Perspectives*
1360 *Letters* **8**, 7-21 (2018).
- 1361 136 Kogarko, L. N., Henderson, C. M. B. & Pacheco, H. Primary Ca-Rich
1362 Carbonatite Magma and Carbonate-Silicate-Sulfide Liquid Immiscibility in the
1363 Upper-Mantle. *Contrib Mineral Petrol* **121**, 267-274 (1995).
- 1364 137 Schiano, P., Clocchiatti, R., Shimizu, N., Weis, D. & Mattielli, N. Cogenetic
1365 Silica-Rich and Carbonate-Rich Melts Trapped in Mantle Minerals in
1366 Kerguelen Ultramafic Xenoliths - Implications for Metasomatism in the
1367 Oceanic Upper-Mantle. *Earth Planet Sci Lett* **123**, 167-178 (1994).
- 1368 138 Dixon, J., Clague David, A., Cousens, B., Monsalve Maria, L. & Uhl, J.
1369 Carbonatite and silicate melt metasomatism of the mantle surrounding the
1370 Hawaiian plume: Evidence from volatiles, trace elements, and radiogenic
1371 isotopes in rejuvenated-stage lavas from Niihau, Hawaii. *Geochemistry,*
1372 *Geophysics, Geosystems* **9**, (2008).
- 1373 139 Rohrbach, A. & Schmidt, M. W. Redox freezing and melting in the Earth's
1374 deep mantle resulting from carbon-iron redox coupling. *Nature* **472**, 209-212,
1375 (2011).
- 1376 140 Dasgupta, R. Volatile-bearing partial melts beneath oceans and continents -
1377 where, how much and of what compositions. *Am J Sci* **318**, 141-165 (2018).
- 1378 141 Eguchi, J. & Dasgupta, R. CO₂ content of andesitic melts at graphite-
1379 saturated upper mantle conditions with implications for redox state of oceanic
1380 basalt source regions and remobilization of reduced carbon from subducted
1381 eclogite. *Contrib Mineral Petrol* **172**, 12, (2017).

- 1382 142 Dalton, J. A. & Presnall, D. C. Carbonatitic melts along the solidus of model
1383 lherzolite in the system CaO-MgO-Al₂O₃-SiO₂-CO₂ from 3 to 7 GPa. *Contrib*
1384 *Mineral Petrol* **131**, 123-135 (1998).
- 1385 143 Dasgupta, R. *et al.* Carbon-dioxide-rich silicate melt in the Earth's upper
1386 mantle. *Nature* **493**, 211-215 (2013).
- 1387 144 Green, D. H. & Wallace, M. E. Mantle Metasomatism by Ephemeral
1388 Carbonatite Melts. *Nature* **336**, 459-462 (1988).
- 1389 145 Keshav, S. & Gudfinnsson, G. H. Melting phase equilibria of model
1390 carbonated peridotite from 8 to 12 GPa in the system CaO-MgO-Al₂O₃-SiO₂-
1391 CO₂ and kimberlitic liquids in the Earth's upper mantle. *Am Mineral* **99**, 1119-
1392 1126 (2014).
- 1393 146 Mysen, B. O. & Boettcher, A. L. Melting of a Hydrous Mantle: I. Phase
1394 Relations of Natural Peridotite at High Pressures and Temperatures with
1395 Controlled Activities of Water, Carbon Dioxide, and Hydrogen. *J Petrol* **16**,
1396 520-548 (1975).
- 1397 147 Wendlandt, R. F. & Mysen, B. O. Melting relations of natural peridotite+CO₂
1398 as a function of degree of partial melting at 15 and 30 kbar. *Am Mineral* **65**,
1399 37-44 (1980).
- 1400 148 Wyllie, P. J. & Huang, W. L. Carbonation and Melting Reactions in System
1401 Cao-Mgo-Sio2-Co2 at Mantle Pressures with Geophysical and Petrological
1402 Applications. *Contrib Mineral Petrol* **54**, 79-107 (1976).
- 1403 149 Yaxley, G. M. & Brey, G. P. Phase relations of carbonate-bearing eclogite
1404 assemblages from 2.5 to 5.5 GPa: implications for petrogenesis of
1405 carbonatites. *Contrib Mineral Petrol* **146**, 606-619 (2004).
- 1406 150 Minarik, W. G. & Watson, E. B. Interconnectivity of Carbonate Melt at Low
1407 Melt Fraction. *Earth Planet Sci Lett* **133**, 423-437 (1995).
- 1408 151 Helffrich, G. R. & Wood, B. J. The Earth's mantle. *Nature* **412**, 501, (2001).
- 1409 152 Dasgupta, R., Hirschmann, M. M. & Smith, N. D. Partial melting experiments
1410 of peridotite + CO₂ at 3 GPa and genesis of alkalic ocean island basalts. *J*
1411 *Petrol* **48**, 2093-2124 (2007).
- 1412 153 Mallik, A. & Dasgupta, R. Reactive Infiltration of MORB-Eclogite-Derived
1413 Carbonated Silicate Melt into Fertile Peridotite at 3 GPa and Genesis of
1414 Alkalic Magmas. *J Petrol* **54**, 2267-2300, (2013).
- 1415 154 Mallik, A. & Dasgupta, R. Effect of variable CO₂ on eclogite-derived andesite
1416 and lherzolite reaction at 3 GPa—Implications for mantle source
1417 characteristics of alkalic ocean island basalts. *Geochemistry, Geophysics,*
1418 *Geosystems* **15**, 1533-1557 (2014).
- 1419 155 Guillot, B. & Sator, N. Carbon dioxide in silicate melts: A molecular dynamics
1420 simulation study. *Geochim Cosmochim Acta* **75**, 1829-1857 (2011).
- 1421 156 Morizet, Y. *et al.* Towards the reconciliation of viscosity change and CO₂-
1422 induced polymerization in silicate melts. *Chem Geol* **458**, 38-47 (2017).
- 1423 157 Langmuir, C., Klein, E. M. & Plank, T. in *Mantle flow and melt generation at*
1424 *mid-coean ridges Geophysical Monograph Series* (eds J. Phipps-Morgan,
1425 D.K. Blackman, & J.M. Sinton) 183-280 (American Geophysical Union, 1992).
- 1426 158 Ghosh, S., Ohtani, E., Litasov, K. D. & Terasaki, H. Solidus of carbonated
1427 peridotite from 10 to 20 GPa and origin of magnesiocarbonatite melt in the
1428 Earth's deep mantle. *Chemical Geology* **262**, 17-28 (2009).
- 1429 159 Frost, D. J. *et al.* Experimental evidence for the existence of iron-rich metal in
1430 the Earth's lower mantle. *Nature* **428**, 409-412 (2004).

- 1431 160 Rohrbach, A. *et al.* Metal saturation in the upper mantle. *Nature* **449**, 456-458
1432 (2007).
- 1433 161 Harmer, R. E. & Gittins, J. The origin of dolomitic carbonatites: field and
1434 experimental constraints. *J African Earth Sci* **25**, 5-28 (1997).
- 1435 162 Nielsen, T. F. D., Solovova, I. P. & Veksler, I. V. Parental melts of melilitolite
1436 and origin of alkaline carbonatite: Evidence from crystallised melt inclusions,
1437 Gardiner complex. *Contrib Mineral Petrol* **126**, 331-344 (1997).
- 1438 163 Guzmics, T. *et al.* Primary carbonatite melt inclusions in apatite and in K-
1439 feldspar of clinopyroxene-rich mantle xenoliths hosted in lamprophyre dikes
1440 (Hungary). *Miner Petrol* **94**, 225, doi:10.1007/s00710-008-0014-5 (2008).
- 1441 164 Woolley, A. R. & Church, A. A. Extrusive carbonatites: A brief review. *Lithos*
1442 **85**, 1-14, (2005).
- 1443 165 Guzmics, T. *et al.* Carbonatite melt inclusions in coexisting magnetite, apatite
1444 and monticellite in Kerimasi calciocarbonatite, Tanzania: melt evolution and
1445 petrogenesis. *Contrib Mineral Petrol* **161**, 177-196 (2011).
- 1446 166 Zaitsev, A. N. & Keller, J. Mineralogical and chemical transformation of
1447 Oldoinyo Lengai natrocarbonatites, Tanzania. *Lithos* **91**, 191-207 (2006).
- 1448 167 Mitchell, R. H. Carbonatites and carbonatites and carbonatites. *Canadian*
1449 *Mineral* **43**, 2049-2068 (2005).
- 1450 168 Weng, Z., Jowitt, S. M., Mudd, G. M. & Haque, N. A Detailed Assessment of
1451 Global Rare Earth Element Resources: Opportunities and Challenges*. *Econ*
1452 *Geol* **110**, 1925-1952 (2015).
- 1453 169 Harmer, R. E. & Gittins, J. The case for primary, mantle-derived carbonatite
1454 magma. *J Petrol* **39**, 1895-1903 (1998).
- 1455 170 Watkinson, D. H. & Wyllie, P. J. Experimental Study of the Composition Join
1456 NaAlSiO₄-CaCO₃-H₂O and the Genesis of Alkalic Rock—Carbonatite
1457 Complexes. *J Petrol* **12**, 357-378 (1971).
- 1458 171 Neumann, E. R., Wulff-Pedersen, E., Pearson, N. J. & Spencer, E. A. Mantle
1459 xenoliths from Tenerife (Canary Islands): Evidence for reactions between
1460 mantle peridotites and silicic carbonatite melts inducing Ca metasomatism. *J*
1461 *Petrol* **43**, 825-857 (2002).
- 1462 172 Klein-BenDavid, O. *et al.* High-Mg carbonatitic microinclusions in some
1463 Yakutian diamonds--a new type of diamond-forming fluid. *Lithos* **112**, 648-659
1464 (2009).
- 1465 173 Kjarsgaard, B. & Peterson, T. Nephelinite-carbonatite liquid immiscibility at
1466 Shombole volcano, East Africa: Petrographic and experimental evidence.
1467 *Miner Petrol* **43**, 293-314 (1991).
- 1468 174 Guzmics, T., Zajacz, Z., Mitchell, R. H., Szabó, C. & Wälle, M. The role of
1469 liquid-liquid immiscibility and crystal fractionation in the genesis of carbonatite
1470 magmas: insights from Kerimasi melt inclusions. *Contrib Mineral Petrol* **169**,
1471 (2015).
- 1472 175 Weidendorfer, D., Schmidt, M. W. & Mattsson, H. B. Fractional crystallization
1473 of Si-undersaturated alkaline magmas leading to unmixing of carbonatites on
1474 Brava Island (Cape Verde) and a general model of carbonatite genesis in
1475 alkaline magma suites. *Contrib Mineral Petrol* **171**, 43 (2016).
- 1476 176 Woolley, A. R. & Kjarsgaard, B. Carbonatite occurrences of the world: map
1477 and database. *Geological Survey of Canada* (2008).
- 1478 177 Jelsma, H., Barnett, W., Richards, S. & Lister, G. Tectonic setting of
1479 kimberlites. *Lithos* **112**, 155-165 (2009).

1480 178 Woolley, A. R. & Bailey, D. K. The crucial role of lithospheric structure in the
1481 generation and release of carbonatites: geological evidence. *Mineral Mag* **76**,
1482 259-270 (2012).

1483 179 Bell, K. & Tilton, G. R. Nd, Pb and Sr isotopic compositions of east African
1484 carbonatites: Evidence for mantle mixing and plume inhomogeneity. *J Petrol*
1485 **42**, 1927-1945 (2001).

1486 180 Bailey, D. K. Episodic alkaline igneous activity across Africa: implications for
1487 the causes of continental break-up. *Geological Society of London Special*
1488 *Publications* **68**, 91-98 (1992).

1489 181 Bell, K. Carbonatites: relationships to mantle-plume activity. *Geological*
1490 *Society of America Special Paper*, 267-290 (2001).

1491 182 Ernst, R. E. & Bell, K. Large igneous provinces (LIPs) and carbonatites.
1492 *Miner Petrol* **98**, 55-76 (2010).

1493 183 Jelsma, H., Barnett, W., Richards, S. & Lister, G. Tectonic setting of
1494 kimberlites. *Lithos* **112**, 155-165 (2009).

1495 184 Hoernle, K., Tilton, G., Le Bas, M. J., Duggen, S. & Garbe-Schonberg, D.
1496 Geochemistry of oceanic carbonatites compared with continental
1497 carbonatites: mantle recycling of oceanic crustal carbonate. *Contrib Mineral*
1498 *Petrol* **142**, 520-542 (2002).

1499 185 Holm, P. M. *et al.* Sampling the cape verde mantle plume: Evolution of melt
1500 compositions on Santo Antao, Cape Verde Islands. *J Petrol* **47**, 145-189
1501 (2006).

1502 186 Schmidt, M. W. & Weidendorfer, D. Carbonatites in oceanic hotspots.
1503 *Geology* **46**, 435-438 (2018).

1504 187 Keshav, S. & Gudfinnsson, G. H. Experimentally dictated stability of
1505 carbonated oceanic crust to moderately great depths in the Earth: Results
1506 from the solidus determination in the system CaO-MgO-Al₂O₃-SiO₂-CO₂.
1507 *Journal of Geophysical Research B: Solid Earth* **115** (2010).

1508 188 Grassi, D. & Schmidt, M. W. The melting of carbonated pelites from 70 to 700
1509 km depth. *J Petrol* **52**, 765-789 (2011).

1510 189 Katsura, T., Yoneda, A., Yamazaki, D., Yoshino, T. & Ito, E. Adiabatic
1511 temperature profile in the mantle. *Phys Earth Planet In* **183**, 212-218 (2010).

1512 190 Hirschmann Marc, M. Mantle solidus: Experimental constraints and the effects
1513 of peridotite composition. *Geochemistry, Geophysics, Geosystems* (2000).

1514 191 Yasuda, A., Fujii, T. & Kurita, K. Melting relations of an anhydrous mid-ocean
1515 ridge basalt from 3 to 20 GPa: Implications for the behaviour of subducted
1516 oceanic crust in the mantle. *J Geophys Res* **99**, 9401-9414 (1994).

1517 192 Day, H. W. A revised diamond-graphite transition curve. *Am Mineral* **97**
1518 (2012).

1519 193 Herzberg, C. & Gazel, E. Petrological evidence for secular cooling in mantle
1520 plumes. *Nature* **458**, 619 (2009).

1521 194 Herzberg, C. *et al.* Temperatures in ambient mantle and plumes: Constraints
1522 from basalts, picrites, and komatiites. *Geochem Geophys Geosys* **8**, - (2007).
1523